

## Cover Letter

Dear editor,

We have carefully addressed the thoughtful comments of the reviewers and believe that our manuscript is now much improved and ready for publication in ACP. In our paper, we present a methodology to infer CO<sub>2</sub> emissions from power plants using satellite observations of co-emitted NO<sub>2</sub>. Reliable estimates of emissions of this important climate gas are necessary for predicting climate change and developing effective mitigation strategies.

Our work is timely as 1) it is currently not feasible to infer CO<sub>2</sub> emissions directly from satellite observations of CO<sub>2</sub> with current sensors, and 2) CO<sub>2</sub> emissions are not reliably measured (at stack) and reported for most power plants around the world. We demonstrated our methodology on eight US power plants. Though we were limited by current (OMI) sensor capabilities, we fully expect that our methodology will be more broadly applied to global power plants using improved NO<sub>2</sub> data from new and upcoming sensors (TROPOMI, TEMPO), which have improved signal-to-noise, finer spatial resolutions, etc.

I am looking forward to hearing from you.

Best regards,  
Fei

Anonymous Referee #1

General comments

The manuscript presents a methodology to derive CO<sub>2</sub> emissions using satellite-based NO<sub>2</sub> retrievals from OMI instrument. The topic is very interesting as not many studies have successfully attempted space-based CO<sub>2</sub> emission estimation (while much more common is the top-down emission estimation for short-lived gases such as NO<sub>2</sub>) and most of the previous studies only derive emissions for a few sites in the world. The results could be a good addition to the existing literature on the subject but I feel this work still does not dramatically improve what was achieved in previous studies in terms of emission estimation from CO<sub>2</sub> point sources. The methodology is reasonable but more effort should be put in proving how this approach could be extended to more than the 8 point sources analysed in the manuscript.

Therefore I would suggest to provide some sort of recommendations (or criteria) on how to apply the same approach to other point sources depending on the characteristics of the power plants. One possibility could be to test the approach on a few other cases outside US in addition to Matimba in order to illustrate the potential differences.

The manuscript can be published after addressing this issue and the following comments.

**Response:** We thank Referee #1 for the thoughtful comments. We have added Figure 8 to compare the US ratios derived in this study with the ratios for other countries from a bottom-up emission database. We have added Figure 9 to further clarify how to apply our approach to power plants outside the US. We have added a new subsection 3.3.1 to discuss the addition.

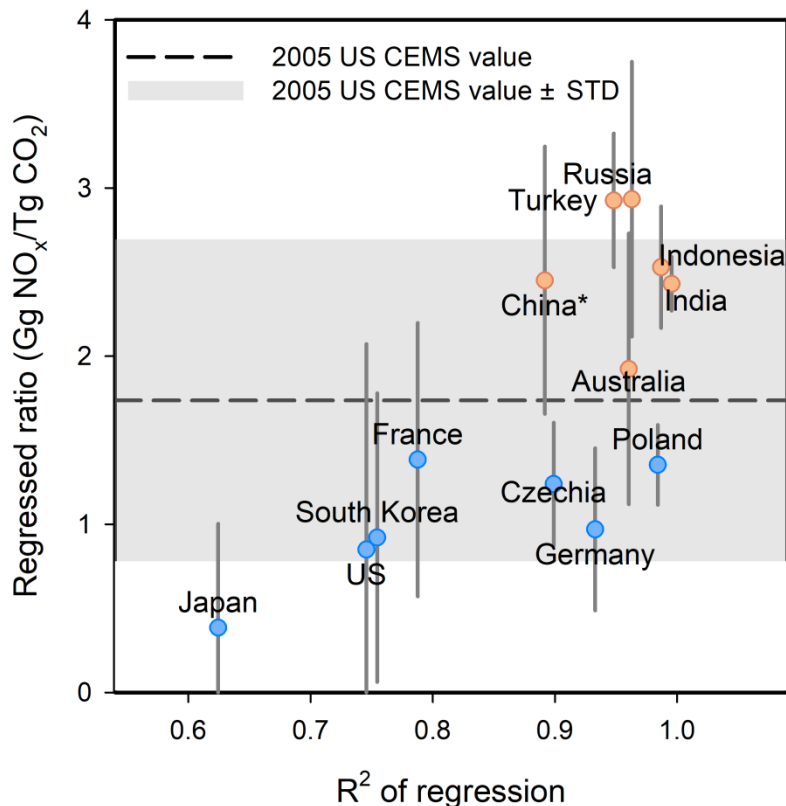


**Figure 8** Comparison of the regressed  $\text{NO}_x$  to  $\text{CO}_2$  emission ratios derived from the global power emissions database (GPED) for different regions versus the correlation coefficient of the regression. The blue and red circles denote regions that are subject to more strict standard for  $\text{NO}_x$  emissions from power plants (i.e., a  $\text{NO}_x$  ELV of  $200 \text{ mg/m}^3$  or less) and other regions, respectively. Y axis: the slope of the regression of the  $\text{NO}_x$  to  $\text{CO}_2$  emissions with an assumed y-intercept of zero. Error bars show the standard deviations for the  $\text{NO}_x$  to  $\text{CO}_2$  emission ratios for individual power plants. X axis: correlation coefficient of the regression. The dashed line represents 2005 US  $ratio_{regressed}^{CEMS}$  for bituminous coal derived in this study. The grey shadow represents 2005 US  $ratio_{regressed}^{CEMS} \pm \text{standard deviation}$ .

\*China switched from being a less strict country to a more strict country in 2014, when most coal-fired power plants in China were required to comply with its new emission standards (GB13223-2011).

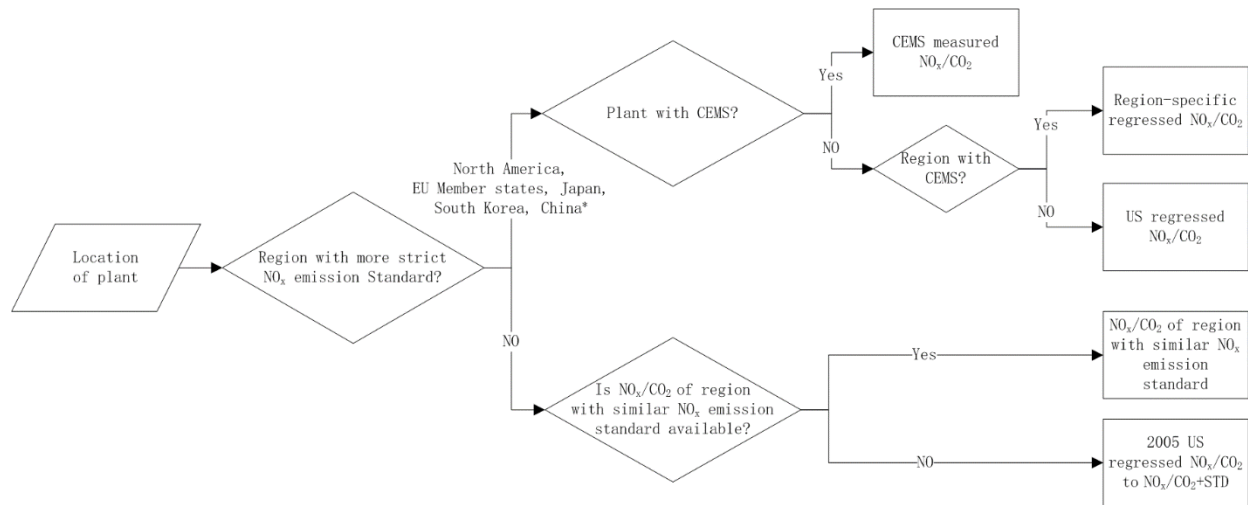


**Figure 9** Schematic of our methodology to estimate the  $\text{NO}_x$  to  $\text{CO}_2$  emission ratios for power plants outside the US.

\*China switched from being a less strict country to a more strict country in 2014, when most coal-fired power plants in China were required to comply with its new emission standards (GB13223-2011).

To better place the importance of our work into context, we added the following paragraph to the conclusions:

“We found that it is feasible to infer  $\text{CO}_2$  emissions from satellite  $\text{NO}_2$  observations, but limitations of the current satellite data (e.g., spatio-temporal resolution, signal-to-noise) only allow us to apply our method to eight large and isolated U.S. power plants. Looking forward, we anticipate that these limitations will diminish for the recently launched (October 2017) European Union Copernicus Sentinel 5 precursor TROPOMI, and three upcoming (launches expected in the early 2020s) geostationary instruments (NASA TEMPO; European Space Agency and Copernicus Programme Sentinel-4; Korea Meteorological Administration Geostationary Environment Monitoring Spectrometer, GEMS), which are designed to have superior capabilities to OMI. For example, higher spatial and temporal resolutions will likely improve the estimation

of NO<sub>x</sub> emissions as well as allow for the separation of more power plant plumes from nearby sources, thus increasing the number of power plants available for analysis. Therefore, future work will be to apply our method to these new datasets, especially after several years of vetted data become available. Additional future work will include applying our ratio-regression method to other regions of the world with reliable CEMS information, such as Europe, Canada and, more recently, China, to develop a more reliable and complete database with region-specific ratios.”

#### *Specific comments*

1. P2 L33 -> *There is a recent update to this paper where the anomalies are calculated on global scale and also TROPOMI data are used for comparison on local scale. You might want to add this as well in your intro: Hakkarainen, J.; Ialongo, I.; Maksyutov, S.; Crisp, D. Analysis of Four Years of Global XCO<sub>2</sub> Anomalies as Seen by Orbiting Carbon Observatory-2. Remote Sens. 2019, 11, 850.*

*Here also another work it might be worth mentioning: Wang, S., Zhang, Y., Hakkarainen, J., Ju, W., Liu, Y., Jiang, F., & He, W. (2018). Distinguishing anthropogenic CO<sub>2</sub> emissions from different energy intensive industrial sources using OCO-2 observations: A case study in northern China. Journal of Geophysical Research: Atmospheres, 123, 9462–9473. <https://doi.org/10.1029/2018JD029005>*

**Response:** We thank for the comments. We have added both references in the introduction of the revised manuscript.

2. P7 L19-20 *“We assume the NO<sub>x</sub> to CO<sub>2</sub> emission ratio of Matimba is on the upper end of the US values, considering that it is not equipped with any NO<sub>x</sub> control devices, even low-NO<sub>x</sub> burners which are widely installed in US power plants” This step is quite critical if you think about extending the method to other sources. You are basically saying that you have to know already something on the source before applying the method. . . how do you expect to make this choice for other sources? Please comment.*

**Response:** The aim of the method developed by this study is to simplify the information needed to derive the NO<sub>x</sub> to CO<sub>2</sub> ratio. The basic information needed for the method is generally available. We have clarified this in Section 3.3.1, as follows:

“The application of the method contributes to simplifying the information needed to derive a reasonable NO<sub>x</sub> to CO<sub>2</sub> emission ratio. In a bottom-up approach, we often need many details including coal type, coal quality, boiler firing type, NO<sub>x</sub> emission control device type, and operating condition of boiler and emission control device when calculating NO<sub>x</sub> and CO<sub>2</sub> emissions. As demonstrated in Section 2.2, the method developed in this study can derive a reasonable estimate of the ratio for power plants without post-combustion NO<sub>x</sub> control device by merely given coal type. Even for regions without reliable emission information, the information on coal type, particularly for large power plants, are very likely publicly available. For power plants installing post-combustion NO<sub>x</sub> control technology, we additionally require the removal efficiency of the device to derive the ratio. The removal efficiency of post-combustion NO<sub>x</sub> control devices is usually directly reported, as the operation of such devices is very expensive and is expected to be subject to strict quality control and assurance standards. ”

3. Fig. 8 How do your emission estimates for Matimba compare with Reuter 2019 estimate?

**Response:** Our estimate for Matimba (including the nearby Medupi which has operated since 2015) is comparable to Reuter 2019 estimate. Our estimate is 1.9–3.0 Gg/h for 2016\* (i.e., the period from 2015 to 2017); Reuter 2019 estimate is  $3.5 \pm 0.8$  Gg/h for 2018. It should be noted that the Medupi power plant started operation in 2015 with limited capacity and that it still has not reached its nominal capacity. Therefore, it is no surprise that our estimate is lower than Reuter 2019 estimate. We have added Reuter 2019 estimate in Figure 11 and the related discussion in Section 3.3.2, as follows:

“Figure 11 shows  $E_{CO_2}^{Sat}$  derived in this study and other independent estimates reported in the literature, including two top-down (Nassar et al., 2017; Reuter et al., 2019) and three bottom-up estimates (Wheeler and Ummel, 2008; Tong et al., 2018; Oda et al., 2018). Despite the uncertainties associated with each of these methods, the CO<sub>2</sub> emissions estimates agree reasonably well.”

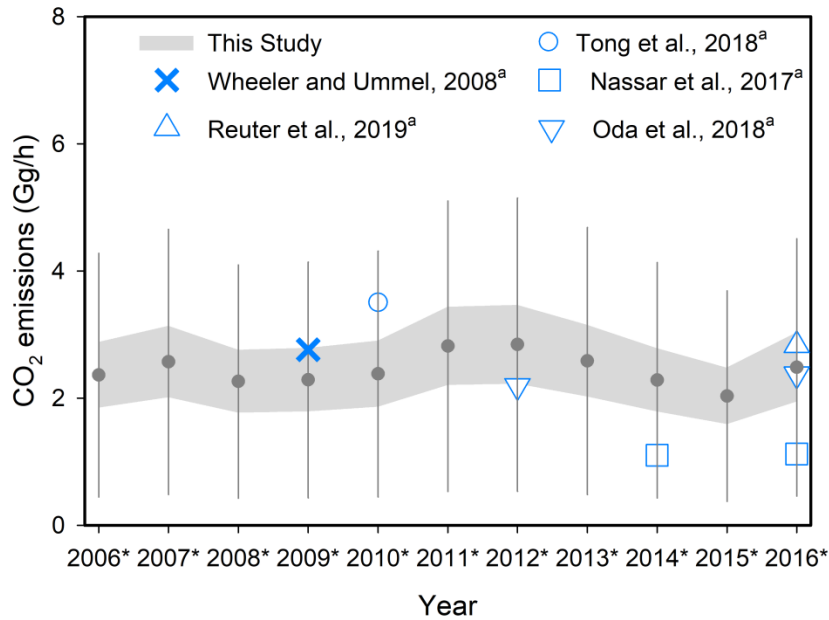


**Figure 11** Comparison of  $E_{CO_2}^{Sat}$  (Gg/h) derived in this study with existing estimates for the Matimba power plant during 2005 to 2017.  $E_{CO_2}^{Sat}$  is inferred based on the NO<sub>x</sub> to CO<sub>2</sub> emissions ratio ranging from  $ratio_{regressed}^{CEMS}$  to  $ratio_{regressed}^{CEMS} +$  standard deviation of ratio. The upper and lower grey bands denote the emissions inferred from  $ratio_{regressed}^{CEMS}$  and  $ratio_{regressed}^{CEMS} +$  standard deviation of ratio, respectively. The grey dots and error bars show the mean of the upper and lower grey bands and their uncertainties, respectively.

<sup>a</sup>Emissions are estimated for 2009 by Wheeler and Ummel (2008); for 2010 by Tong et al. (2018); for 2014 and 2016 by Nassar et al. (2017); for 2016 by Reuter et al. (2019); and for 2012 and 2016 by Oda et al. (2018).

4. P11 L25 This paper is now published: Reuter, M., Buchwitz, M., Schneising, O., Krautwurst, S., O'Dell, C. W., Richter, A., Bovensmann, H., and Burrows, J. P.: Towards monitoring localized CO<sub>2</sub> emissions from space: co-located regional CO<sub>2</sub> and NO<sub>2</sub> enhancements observed by the OCO-2 and S5P satellites, *Atmos. Chem. Phys.*, 19, 9371-9383, <https://doi.org/10.5194/acp-19-9371-2019>, 2019.

**Response:** Thanks for pointing out this. We have updated the reference in the revised manuscript.

5. Sect. 2.2 Is there any other dataset in addition to EPA's CEMS you could verify these ratios with?

**Response:** EPA's CEMS has been widely used to develop emission inventories. To the best of our knowledge, all the widely-used regional and global bottom-up emission inventories adopt EPA's CEMS to estimate NO<sub>x</sub> and CO<sub>2</sub> emissions for US power plants. To the best of our knowledge, there is no independent dataset available to verify the derived ratios for the US power plants.

Technical comments

P3 L20 “. . .plants.As discussed” there is a space missing here

**Response:** Thanks for pointing out this. We have updated it in the revised manuscript.

P7 L11 I would change the title with “Application to Matimba power plant” or something like that more specific

**Response:** Thanks. We have changed the title for section 3.3.2 accordingly.

*Anonymous Referee #2*

*Liu et al. describe a method to estimate CO<sub>2</sub> emissions from power plants using satellite observations of tropospheric NO<sub>2</sub> columns. The method involves the estimation of NO<sub>x</sub> emissions using a top-down approach previously developed by the authors and estimation of CO<sub>2</sub> emissions by applying a NO<sub>x</sub>/CO<sub>2</sub> emission ratio derived from direct stack emission measurements of both gases. The topic of the manuscript is important and relevant in the context of the ongoing development of the global emission monitoring system intended to support the elaboration of climate control and mitigation strategies. Although the idea to use satellite NO<sub>2</sub> measurements to constrain CO<sub>2</sub> emissions from fossil fuel burning is not new, application of this approach to specifically power plant emissions is a step forward. Another new point of the study is the analysis of the relationship between NO<sub>x</sub> and CO<sub>2</sub> emissions from different types of coal-fired power plants in the US. That said, I keep wondering whether and how the method proposed in this manuscript can be proven useful in any scientific or practical applications. The weak points of the manuscript and my suggestions to the authors are outlined in my comments below.*

**Response:** We thank Referee #2 for the thoughtful comments, which we address carefully below.

Major comment

*I find that the manuscript lacks clear logic in presenting the ideas and results of the authors. Specifically, while the main focus in Section 2 (“Method”) is given to the analysis of the CEMS stack measurements in the US in the period from 2005 to 2017, it is not explained and justified how the outcome of this analysis can be used for applications outside of the US. Such possible applications are illustrated in the manuscript (in Sect. 3.3) by the example of only one power plant (Matimba), for which the authors use the NO<sub>x</sub>/CO<sub>2</sub> emission ratio estimated only for 2005 and even argue that this estimate (based on the US data) is not directly applicable to the Matimba plant. Furthermore, if the “regressed” estimates of the NO<sub>x</sub>/CO<sub>2</sub> emission ratio are not directly applicable to power plants outside of the US, the application of these approximate estimates to the selected 8 power plants inside of the US (presumably to test the method) seems to be pointless, as the CEMS measurements provide accurate direct estimates of the NO<sub>x</sub>/CO<sub>2</sub> emission ratio for any power plant in the US. As for the Matimba power plant, a reasonable alternative to using the CEMS measurements would be to get a corresponding estimate of the NO<sub>x</sub>/CO<sub>2</sub> emission ratio from the ODIAC inventory. Therefore, in the present form, the discussion and evaluation of the method is very confusing and, to some extent, misleading. In this respect, I recommend that the authors illustrate the potential of their method and the usefulness of the analysis of the US CEMS data by considering a few more power plants outside of the US (e.g., in China), paying special attention to the accuracy of the estimates of the NO<sub>x</sub>/CO<sub>2</sub> emission ratio based on the US CEMS data versus the accuracy of corresponding estimates that can be obtained directly from available data of global and regional emission inventories.*

**Response:** We address the major comment as below.

- The significance of the method validation for US power plants:

In our study, we investigate the feasibility of using satellite data of NO<sub>2</sub> to infer CO<sub>2</sub> emissions, which could serve as a complementary verification of bottom-up inventories or be used to supplement these inventories.

We first apply our methodology to U.S. power plants, which have accurate CEMS emissions. We systematically identify sources of variation (i.e., coal type and type of NO<sub>x</sub> control device). The

high degree of accuracy of the U.S. CEMS data allows us to verify whether our methodology is feasible or not. In short, we found that it is feasible, but limitations of the current satellite data (e.g., spatio-temporal resolution, signal-to-noise) only allow us to apply our methodology to eight power plants.

Looking forward, we anticipate that current (e.g., TROPOMI) and future sensors (e.g., TEMPO, Sentinel-4, GEMS) will reduce the limitations of the satellite data, especially after their time records have lengthened, allowing us to apply our methodology to more the US and world power plants.

We have clarified this in the revised abstract, introduction and conclusion.

- The potential application of the method and the US ratio derived in this study:

CEMS measurements are available for some power plants in the US, Canada, European Union (EU) member states, Japan, South Korea, and, more recently, China. However, there is still a significant number of power plants in those countries without CEMS technology, particularly for CO<sub>2</sub> measurements. For example, EU member states do not require power plants to use CEMS for CO<sub>2</sub> reporting and the majority of plants in the EU therefore reports CO<sub>2</sub> emissions based on emission factors (Sloss, 2011). Therefore, we recommend applying our method described in Section 2.2 to infer region-specific ratios for those power plants. The method developed in this study provides a simplified but reliable method to determine the ratios for those power plants.

Many or most power plants in South America, Africa, and Asia (minus China) do not report CEMS measurements at all or their observations are of questionable quality. Therefore, bottom-up emission inventories for NO<sub>x</sub> and CO<sub>2</sub> from these countries are highly uncertain, confounding national and international efforts to design effective climate mitigation strategies. We have added a new subsection 3.3.1 to discuss how to apply the ratios derived in this study to other regions.

As suggested, we added the comparison of the ratios derived in this study with those in the global coal-fired power plant emissions database (GPED) in Section 3.3.1. GPED is the only publicly available bottom-up emission database reporting both NO<sub>x</sub> and CO<sub>2</sub> emissions for individual power plants all over the world. The US values show reasonable agreement with other countries' values identified by GPED. The details are as follows:

“Figure 8 shows the NO<sub>x</sub> to CO<sub>2</sub> emission ratios for 2010 from the global power emissions database (GPED; Tong et al., 2018), which is the only publicly-available bottom-up emission database that reports both NO<sub>x</sub> and CO<sub>2</sub> emissions for individual power plants for every country. All countries with over 30 coal-fired power plants in GPED are shown in Figure 8. Not surprisingly, countries with more strict standards in place for NO<sub>x</sub> emissions from power plants (i.e., NO<sub>x</sub> emission limit value (ELV) < 200 mg/m<sup>3</sup>; hereafter referred to as “more strict countries”) have smaller NO<sub>x</sub> to CO<sub>2</sub> ratios (i.e., 1.0 versus 2.5 on average) than countries with less strict standard (i.e., NO<sub>x</sub> ELV > 200 mg/m<sup>3</sup>; hereafter referred to as “less strict countries”). Additionally, the correlation coefficients are smaller for more strict countries (i.e., 0.82 on average) as compared to less strict countries (i.e., 0.96 on average), because power plants in more strict countries are more likely to have installed post-combustion NO<sub>x</sub> control systems, which likely lowered  $ratio_y^{CEMS}$ , similar to what occurred in the US over our analysis period (Section 2.2.2).

We further compare the 2005 US  $ratio_{regressed}^{CEMS}$  in Table 1 with the GPED NO<sub>x</sub> to CO<sub>2</sub> emission ratios for less strict countries. We chose the 2005 value for comparison based on the following considerations. In 2005, the US EPA issued the Clean Air Interstate Rule (CAIR) to address the interstate transport of ozone and fine particulate matter pollution for eastern US states, which reduced NO<sub>x</sub> emissions and, thus, NO<sub>x</sub> to CO<sub>2</sub> ratios ( $ratio_y^{CEMS}$ ). However, similar comprehensive control strategies have not been adopted



in less strict countries. In this way, the 2005 values are expected to show better consistency with the NO<sub>x</sub> to CO<sub>2</sub> ratios of less strict countries than values for more recent years. Note that the GPED database does not give information on ratios by coal type. Therefore, we use  $ratio_{regressed}^{CEMS}$  for bituminous coal, which is the most widely used coal type in coal-fired power plants in most countries.

The ratios for individual power plants in less strict countries tend to be larger than the US  $ratio_{regressed}^{CEMS}$  for 2005, considering that power plants in those countries may not be equipped with any NO<sub>x</sub> control devices or even low-NO<sub>x</sub> burners, a technology which is widely installed in US power plants with and without post-combustion NO<sub>x</sub> control devices. Most ratios range from US 2005  $ratio_{regressed}^{CEMS}$  to 2005  $ratio_{regressed}^{CEMS}$  + standard deviation (Figure 8). It is no surprise that some less strict countries have ratios higher than this range, which also occurs for some US power plants without post-combustion emission controls (Figure 4). However, there are considerable uncertainties in the GPED database given the scarcity of reliable emissions information in less strict countries. For example, the GPED NO<sub>x</sub> and CO<sub>2</sub> emissions estimates for Turkey and Russia, which are outliers in Figure 8, are subject to more assumptions and, thus, larger uncertainties than countries with high-quality country-specific emission data, such as China, which has a high-resolution emissions database (CPED; Liu et al., 2015), and India, which has a database developed by Argonne National Laboratory (Lu et al., 2011).

Figure 9 shows a schematic of our methodology to estimate the NO<sub>x</sub> to CO<sub>2</sub> emission ratios for power plants outside the US. We adopt different approaches for more and less strict countries. More strict countries, including Canada, European Union (EU) member states, Japan, South Korea, and, more recently, China, usually use CEMS to monitor emissions, particularly from the largest emitters. For power plants with CEMS measurements for both NO<sub>x</sub> and CO<sub>2</sub> emissions, it is straightforward to use the measured ratios. However, there is still a significant number of power plants in those countries without CEMS technology, particularly for CO<sub>2</sub> measurements. For example, EU member states do not required power plants to use CEMS for CO<sub>2</sub> reporting and the majority of plants in the EU therefore reports CO<sub>2</sub> emissions based on emission factors (Sloss, 2011). Therefore, we recommend applying our method described in Section 2.2 to infer region-specific ratios for those power plants. The US  $ratio_{regressed}^{CEMS}$  could be a less accurate, but reasonable approximation when no CEMS data are available, considering those countries share similar NO<sub>x</sub> ELVs for power plants as the US. For less strict countries, we recommend using the 2005 US values by coal type when ratios from countries with similar NO<sub>x</sub> emission standard are not available. We also recommend assigning a range from 2005  $ratio_{regressed}^{CEMS}$  to 2005  $ratio_{regressed}^{CEMS}$  + standard deviation, instead of a fixed value, to the ratio for inferring CO<sub>2</sub> emissions, considering the knowledge on ratios from those regions are too few to narrow the constraint.

As demonstrated in Section 2.2, our method presented in this study provides a reasonable estimate of the ratio for power plants without post-combustion NO<sub>x</sub> control devices with only knowing coal type. Even for regions without reliable emission information, the information on coal type, particularly for large power plants, are very likely publicly-available. For power plants that install post-combustion NO<sub>x</sub> control technology, we additionally require the removal efficiency of the device to derive the ratio. The removal efficiency of post-combustion NO<sub>x</sub> control devices is usually directly reported, as the operation of such devices is very expensive and is expected to be subject to strict quality control and assurance standards. In contrast to bottom-up approaches, many details are required, including coal type, coal quality, boiler firing type, NO<sub>x</sub> emission control device type, and operating condition of boiler and

emission control device, when calculating NO<sub>x</sub> and CO<sub>2</sub> emissions.”

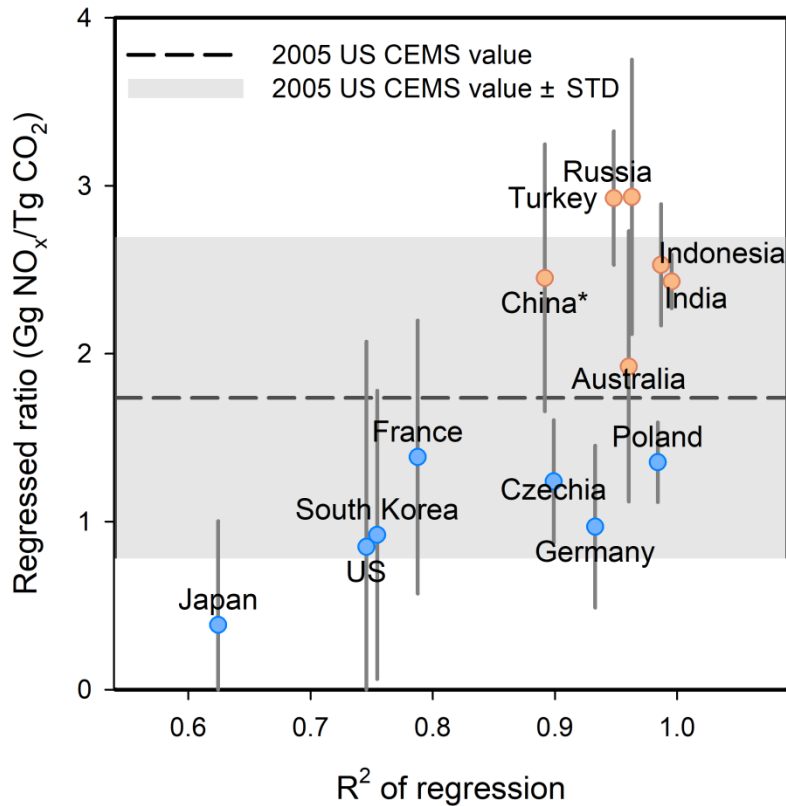


**Figure 8** Comparison of the regressed NO<sub>x</sub> to CO<sub>2</sub> emission ratios derived from the global power emissions database (GPED) for different regions versus the correlation coefficient of the regression. The blue and red circles denote regions that are subject to more strict standard for NO<sub>x</sub> emissions from power plants (i.e., a NO<sub>x</sub> ELV of 200 mg/m<sup>3</sup> or less) and other regions, respectively. Y axis: the slope of the regression of the NO<sub>x</sub> to CO<sub>2</sub> emissions with an assumed y-intercept of zero. Error bars show the standard deviations for the NO<sub>x</sub> to CO<sub>2</sub> emission ratios for individual power plants. X axis: correlation coefficient of the regression. The dashed line represents 2005 US  $ratio_{regressed}^{CEMS}$  for bituminous coal derived in this study. The grey shadow represents 2005 US  $ratio_{regressed}^{CEMS} \pm$  standard deviation.

\*China switched from being a less strict country to a more strict country in 2014, when most coal-fired power plants in China were required to comply with its new emission standards (GB13223-2011).

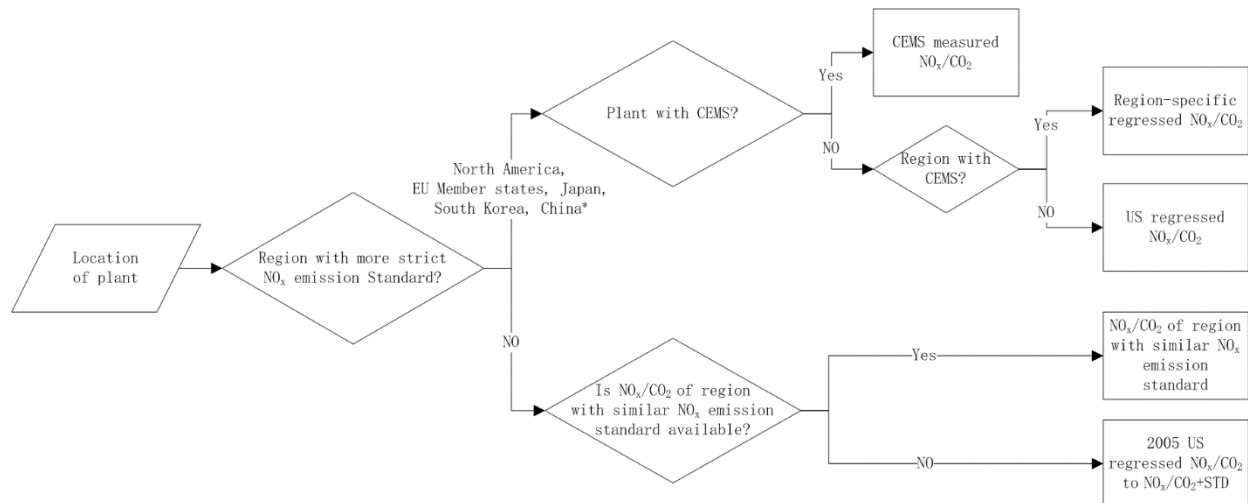


**Figure 9** Schematic of our methodology to estimate the  $\text{NO}_x$  to  $\text{CO}_2$  emission ratios for power plants outside the US.

\*China switched from being a less strict country to a more strict country in 2014, when most coal-fired power plants in China were required to comply with its new emission standards (GB13223-2011).

- The recommendation of using the ODIAC inventory to derive the ratios.

We agree that ODIAC is a great source for  $\text{CO}_2$  emissions. However, it does not provide  $\text{NO}_x$  emissions. It is not practical to calculate the ratios based on ODIAC.

#### *Specific comments*

*p.2, l.16-18: I believe that the narrow swath of the OCO-2 sensor is not the main reason for the limitations of the novel and promising method proposed by Reuter et al. (2019). I suggest that the authors provide a more extensive and accurate discussion (not necessarily in Introduction) of the advantages and disadvantages of their approach with respect to that of Reuter et al. (2019).*

**Response:** We have added the discussion in the revised introduction, as follows:

“More recently, the co-located regional enhancements of  $\text{CO}_2$  observed by OCO-2 and  $\text{NO}_2$  observed by TROPOMI were analysed to infer localized  $\text{CO}_2$  emissions for six hotspots including one power plant globally (Reuter et al., 2019). As emissions plumes are significantly longer than the swath width of OCO-2 (10km), OCO-2 sees only cross sections of plumes, which may not be sufficient to infer emission strengths. Because power plant emissions can have substantial temporal variations (Velazco et al., 2011) and the cross-sectional  $\text{CO}_2$  fluxes are valid only for OCO-2 overpass times, the cross-sectional fluxes may not adequately represent the annual or monthly averages, which are required for the development of climate mitigation strategies. In addition, the cross-sectional fluxes may not be a good approximation for emission strengths if meteorological conditions are not taken into account (Varon et al., 2018). As compared to the method proposed in this study, Reuter’s method has the advantage of not requiring a priori emission information. However, there are currently no satellite instruments with a wide enough swath to allow wider application of Reuter’s method.”

*p.2, l.37: I recommend that the authors avoid boasting about the “novel” method here and elsewhere. Actually, the only significant new point of their method is that it is focused on a*

*particular source of CO<sub>2</sub> emissions (as noted above). A very similar method to constrain CO<sub>2</sub> emissions is described in previous papers (cited in this manuscript) focused on estimating fossil fuel burning CO<sub>2</sub> emissions in China and in Europe. Certainly, there are differences concerning the ways to estimate the NO<sub>x</sub> emissions and NO<sub>x</sub>/CO<sub>2</sub> emission ratio in the different studies, but these differences are mostly of technical nature. Furthermore, the method which was used to estimate NO<sub>x</sub> emissions in this study is identical to that presented by the same authors in their previous papers.*

**Response:** We have deleted the term of novel in the revised manuscript.

*p.3, l.7-12: It would be useful to explain briefly why a special approximation procedure is needed to estimate a NO<sub>x</sub>/CO<sub>2</sub> emission ratio while using the CMES data (i.e. why the NO<sub>x</sub>/CO<sub>2</sub> emission ratio for any given power plant in the US could not be directly evaluated using the corresponding CMES measurements).*

**Response:** CEMS measurements are available for some power plants in the US, Europe, Canada and, more recently, China. For those power plants with CEMS measurements, we agree that it is more straightforward and accurate to use the measured values. However, there is still a significant number of power plants in those countries without CEMS technology, particularly for CO<sub>2</sub> measurements. The method developed by this study provides a more reliable method to determine the ratios for those power plants without CEMS based on CEMS data for other plants. We have clarified this in the revised Section 3.3.1, as follows:

“More strict countries, including Canada, European Union (EU) member states, Japan, South Korea, and, more recently, China, usually use CEMS to monitor emissions, particularly from the largest emitters. For power plants with CEMS measurements for both NO<sub>x</sub> and CO<sub>2</sub> emissions, it is straightforward to use the measured ratios. However, there is still a significant number of power plants in those countries without CEMS technology, particularly for CO<sub>2</sub> measurements. For example, EU member states do not require power plants to use CEMS for CO<sub>2</sub> reporting and the majority of plants in the EU therefore reports CO<sub>2</sub> emissions based on emission factors (Sloss, 2011). Therefore, we recommend applying our method described in Section 2.2 to infer region-specific ratios for those power plants. The US  $ratio_{regressed}^{CEMS}$  could be a less accurate, but reasonable approximation when no CEMS data are available, considering those countries share similar NO<sub>x</sub> ELVs for power plants as the US.”

*P3. l.21. It is quite unusual and inconvenient that the first figure ever mentioned in the manuscript is Figure 5 (instead of Figure 1). The order of the figures should be corrected.*

**Response:** Thanks. We have reordered the figures in the revised manuscript.

*p.3, l.29-32: The authors should explain the origin and significance of the value “1.32”. Would their estimates be less accurate if they assumed that the NO<sub>x</sub>/NO<sub>2</sub> ratio equals, say, to 1.3? Further, do the authors imply that if one had a way to measure the NO/NO<sub>2</sub> ratio around any power plant anywhere in the world with a spatial resolution of 13 km×24 km, then the measured NO<sub>x</sub>/NO<sub>2</sub> ratio would be exactly 1.32? Wouldn't the NO<sub>x</sub>/NO<sub>2</sub> ratio actually strongly vary from*

*site to site and would depend on the ozone level (which is frequently not determined by local pollution sources) and the age of the plume? Doesn't the fact that the estimates of the NO<sub>x</sub> lifetime inferred from satellite measurements vary across the 8 power plants within almost a factor of 2 (according to Table 2) mean that OH (and therefore O<sub>3</sub>) levels are quite different in plumes from different power plants? Overall, I believe that the uncertainty associated with the estimation of the NO<sub>x</sub>/NO<sub>2</sub> ratio should be carefully discussed and evaluated (perhaps, using a chemistry transport model). A brief and superficial discussion of this important point in Liu et al. (2016) is certainly insufficient.*

**Response:** The number of 1.32 used for scaling up the NO<sub>2</sub> to NO<sub>x</sub> is based on the typical assumptions made in the section 6.5.1 of Seinfeld and Pandis (2006) for “typical urban conditions and noontime sun” following the recommendation by Beirle et al. (2011). We agree that the NO/NO<sub>2</sub> ratio might vary locally. But these local variations are not expected to be significant over spatial scales of ~100–200 km and annual temporal averaging. We included increased uncertainty of the NO<sub>x</sub>/NO<sub>2</sub> ratio from 10% to 20% when calculating the overall uncertainties. We recognize that uncertainties resulting from the NO<sub>x</sub>/NO<sub>2</sub> ratio may be better understood when more direct measurements are available in the future. We have clarified this in the Section 3.2 of the revised manuscript, as follows:

“The number of 1.32 used for scaling the NO<sub>2</sub> to NO<sub>x</sub> ratio is based on assumptions presented in section 6.5.1 of Seinfeld and Pandis (2006) for “typical urban conditions and noontime sun”. Note that conditions are quite similar in this study because of the overpass time of OMI close to noon, the selection of cloud-free observations, the focus on the ozone season, and the focus on polluted regions. A case study of CTM simulations shows an identical value of 1.32 for Paris in summer (Shaiganfar et al., 2017). The simulated NO<sub>x</sub>/NO<sub>2</sub> ratio at the OMI overpass time within the boundary layer (up to 2 km) in a chemistry–climate model, EMAC (Jöckel et al., 2016), was  $1.28 \pm 0.08$  for polluted (NO<sub>x</sub> >  $1 \times 10^{15}$  molec cm<sup>-2</sup>) regions for the July 1, 2005, and  $1.32 \pm 0.06$  on average for the ozone season. However, the coarse grid of EMAC ( $2.8^\circ \times 2.8^\circ$  in latitude and longitude) may not capture the true range of variation of the NO<sub>x</sub>/NO<sub>2</sub> ratio. Therefore, we assumed an uncertainty of 20% arising from the NO<sub>x</sub>/NO<sub>2</sub> ratio, double than the standard deviation of the EMAC ratio.”

*Table S1: The authors provided some useful supplementary information for Sect. 2.1 in Table S1, but this table is not mentioned and discussed anywhere in the manuscript.*

**Response:** Thanks for pointing out this. We have introduced the table in the revised manuscript, as follows:

“The locations of the 8 plants are shown in Figure 1 and given in Table S1.”

“The fitted lifetimes and other fitting parameters for all power plants are given in Table S1.”

*p.4, l.3-33: I suggest the authors provide an additional figure illustrating the NO<sub>2</sub> plume from the Rockport power plant along with a corresponding Gaussian fit.*

**Response:** Thanks. We have added it as Figure 2 in the revised manuscript.

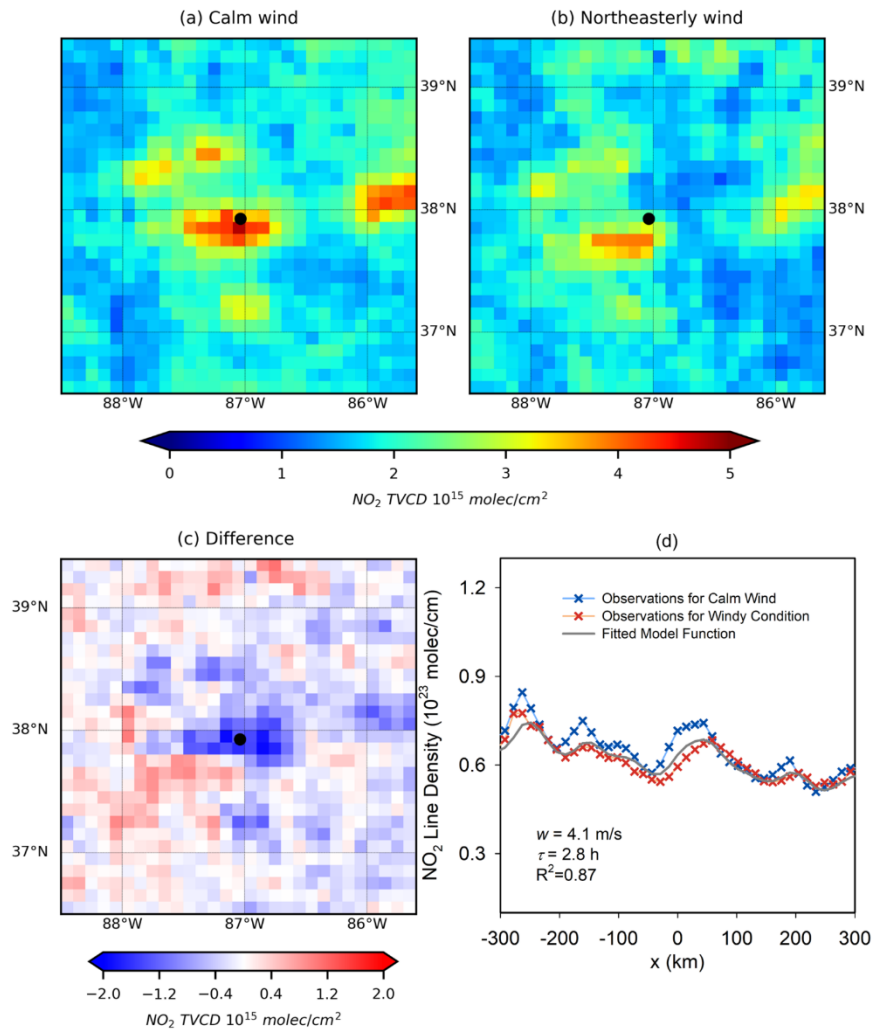


**Figure 2** Mean OMI NO<sub>2</sub> tropospheric VCDs around the Rockport power plant (Indiana, USA) for (a) calm conditions, (b) northeasterly winds and (c) their difference (northeasterly – calm) for the period of 2005 – 2017. The location of Rockport is labelled by a black dot. (d) NO<sub>2</sub> line densities around Rockport. Crosses: NO<sub>2</sub> line densities for calm (blue) and northeasterly winds (red) as function of the distance x to Rockport center. Grey line: the fit result. The numbers indicate the net mean wind velocities (windy – calm) from MERRA-2 (w) and the fitted lifetime  $\tau$ .

p.5, l.5: It would be helpful if the authors explained here what is the purpose of creating “continuous and consistent records of ratio\_CEMS...”. Are these records supposed to be helpful for estimating CO<sub>2</sub> emissions inside of the US (although accurate estimates of the NO<sub>x</sub>/CO<sub>2</sub> ration are already provided by CEMS for each power plant) or outside of the US (although the applicability of the CEMS data outside of the US is very questionable)?

**Response:** The sentence indicates that  $ratio^{CEMS}$  for plants prior to and after installing post-combustion NO<sub>x</sub> control systems is continuous and consistent, because the estimation is based on

$ratio_{regressed}^{CEMS}$  for plants without post-combustion control systems in operation. We have deleted the terms of continuous and consistent in the revised manuscript to prevent misunderstanding.

*Sect. 3.2: In my opinion, the uncertainties of the emission estimates inferred from the OMI measurements are well characterized by the standard deviations reported in Table 3. However, these “data-based” uncertainty estimates are not discussed in the manuscript. The present discussion of the uncertainties, however, looks very superficial. I suggest the authors provide a separate table (e.g., in the Supporting information) reporting the uncertainties associated with each power plant and with each individual factor contributing to the total uncertainty. Also, I wonder how a reader acquainted with the basic knowledge of the mathematical statistics is supposed to interpret the values of the uncertainty reported in this section. Do these values represent the standard deviation (that is, the confidence interval corresponding to the 68.3 percentile)? If so, does the fact that the uncertainty estimates range from 62%–96% mean that there is a significant chance that a true value of the emissions can be below zero (assuming that the error distribution is Gaussian)? My suggestion is to consider reporting the so huge uncertainties in terms of the geometric standard deviation (thus assuming that the error distribution is log-normal).*

**Response:** We agree that the standard deviation reported in Table 3 is a good indicator of the uncertainty. We also calculate the geometric standard deviation of the difference between  $E_{CO_2}^{CEMS}$  and  $E_{CO_2}^{Sat}$  from 2006\* to 2016\* for individual power plants in Table S2 as an alternative measure to reflect the uncertainty following the suggestion of the reviewer. In the revised manuscript, we have added the discussion on this “data-based” uncertainty analysis, as follows:

“The mean and the standard deviation of the relative differences between  $E_{NO_x}^{CEMS}$  and  $E_{NO_x}^{Sat}$ , and  $E_{CO_2}^{CEMS}$  and  $E_{CO_2}^{Sat}$  for all eight power plants provide a good alternative measure of uncertainties (Table 3). The relative differences are rather small, which are  $0\% \pm 33\%$  and  $8\% \pm 41\%$  (mean  $\pm$  standard deviation) for  $NO_x$  and  $CO_2$ , respectively. We additionally calculate the geometric standard deviations (GSDs) of the difference between  $E_{CO_2}^{CEMS}$  and  $E_{CO_2}^{Sat}$  from 2006\* to 2016\* for individual power plants in Table S2. The small values of GSDs ranging from 1.07 to 1.31 further improve our confidence in the accuracy of the derived emissions in this study.”

We have added a separate Table S2 to list the contributors to the overall uncertainties as suggested by the reviewer. We report the derived uncertainties as a 95% confidence interval (CI). Note that we adjust our uncertainty estimates for some contributors. We increased the uncertainty of the  $NO_x/NO_2$  ratio from 10% to 20% (see response to the comments on the  $NO_x/NO_2$  ratio). We decreased the uncertainty arising from the variations of fitted lifetimes by wind direction from 40% to 20%, because the average of the standard deviation of lifetimes for all wind directions decreased from 40% in Liu et al. (2016) to 20% in this study. The details are given in section 1 of the supplement, as follows:

“The uncertainty analysis is similar to the procedure described in our previous work (Liu et al., 2016), based on the fit performance and the dependencies on the a priori settings as determined in sensitivity studies. We report the derived uncertainties as a 95% confidence interval (CI). Here we briefly list the sources of uncertainties and how they are quantified. Further details are provided in Section 3 of the Supplement of Liu et al. (2016). In summary, we conclude that:

- *Choice of integration and fit intervals:* Uncertainties arising from the choice of integration and fit intervals are about 10% for the lifetime and 20% for the total NO<sub>2</sub> mass, respectively, based on our sensitivity analysis by changing integration and fit intervals.
- *Fit errors:* The fit errors expressed as 95% confidence interval (CI) are derived from the least-squares fit routine directly for individual sources. They are typically on the order of 10% for both lifetime and total NO<sub>2</sub> mass, both of which are propagated into the uncertainty of  $E_{NO_x}^{Sat}$ . In addition, the standard deviation of fitted lifetimes for all wind direction sectors is regarded as a measure of uncertainty to reflect the reliability of lifetimes, which is 20% on average for all power plants.
- *Wind fields:* The uncertainty associated with the wind data is 30%. The choice of wind layer height and the uncertainties of wind fields themselves contribute to the overall uncertainty.
- The derived NO<sub>x</sub> emissions are affected by the uncertainty of the NO<sub>2</sub> tropospheric VCDs (~30%) and the NO<sub>x</sub>/NO<sub>2</sub> ratio (~20%).
- Effects of a possible systematic change of NO<sub>2</sub> tropospheric VCDs from calm to windy conditions result in an uncertainty of ~10%.
- $ratio_{regressed}^{CEMS}$  contributes to an uncertainty of 15%.
- For power plants with post-combustion NO<sub>x</sub> control devices, an additional uncertainty of 20% comes from the predicted NO<sub>x</sub> removal efficiency of the devices.

The uncertainties of each contributor for individual power plants are listed in Table S2. We assume that their contributions to the total uncertainty are independent and define the total uncertainty as the root of the quadratic sum of the aforementioned contributions.”

*p.7, l.19,20: If the authors believe that the NO<sub>x</sub>/CO<sub>2</sub> emission ratio at Matimba is on the upper end of the US values, then perhaps they should have used a maximum value of the NO<sub>x</sub>/CO<sub>2</sub> emission ratios among all of the US power plants without NO<sub>x</sub> emission control. Anyway, it is not clear how the standard deviation of ratio<sub>regressed</sub> was evaluated? Is it the standard deviation of the slope of a linear fit or the standard deviation of the original NO<sub>x</sub>/CO<sub>2</sub> emission ratios from the CMES data?*

**Response:** We assume the NO<sub>x</sub> to CO<sub>2</sub> emission ratio of Matimba is on the upper end of the US values, considering South Africa has not implemented improvements in boiler operations to decrease the ratio, such as optimizing furnace design and operating conditions, as in the US. We thus use the ratio for year 2005, instead those for more recent years to infer CO<sub>2</sub> emissions for the entire period. The standard deviation is that of the NO<sub>x</sub>/CO<sub>2</sub> emission ratios for individual power plants from CEMS. We believe the ratio of Matimba is more likely to range from 2005  $ratio_{regressed}^{CEMS}$  to 2005  $ratio_{regressed}^{CEMS} + \text{standard deviation}$ , instead of being 2005  $ratio_{regressed}^{CEMS}$ , considering that it is not equipped with any NO<sub>x</sub> control devices, even low-NO<sub>x</sub> burners which are widely installed in US power plants. But we don't use the maximum value of the ratio in this study, because it may be related with some plant-specific operating conditions, which is not applicable to other plants. We have clarified how to apply the ratios derived in this study to other regions in Section 3.3.1.



*p.7, l.29-31: According to Reuter et al. (2019), the CO<sub>2</sub> emission estimates for the Matiba power plant are available also from the ODIAC inventory. The authors could consider using the corresponding estimates for comparison.*

**Response:** Thanks. We have added the estimates from ODIAC in Figure 11 of the revised manuscript.  $E_{CO_2}^{Sat}$  derived in this study shows reasonable agreement with the ODIAC.

*Conclusions: This section looks unusually short for ACP. Furthermore, instead of providing a clear and logical summary of the major findings of the study, the authors preferred to speculate about possible future developments of their method. Accordingly, I believe this section needs to be re-written and significantly extended.*

**Response:** We have extended the conclusion substantially to provide a summary of the major findings, as follows:

“In our study, we investigated the feasibility of using satellite data of NO<sub>2</sub> from power plants to infer co-emitted CO<sub>2</sub> emissions, which could serve as complementary verification of bottom-up inventories or be used to supplement these inventories that are highly uncertain in many regions of the world. For example, our estimates will serve as an independent check of CO<sub>2</sub> emissions that will be inferred from satellite retrievals of future CO<sub>2</sub> sensors (Bovensmann et al., 2010). Currently, uncertainties in CO<sub>2</sub> emissions from power plants confound national and international efforts to design effective climate mitigation strategies.

We estimate NO<sub>2</sub> and CO<sub>2</sub> emissions during the “ozone season” from individual power plants from satellite observations of NO<sub>2</sub> and demonstrate its utility for US power plants, which have accurate CEMS with which to evaluate our method. We systematically identify the sources of variation, such as types of coal, boiler, and NO<sub>x</sub> emission control device, and change in operating conditions, which affect the NO<sub>x</sub> to CO<sub>2</sub> emissions ratio. Understanding the causes of these variations will allow for better informed assumptions when applying our method to power plants that have no or uncertain information on the factors that affect their emissions ratios. For example, we estimated CO<sub>2</sub> emissions from the large and isolated Matimba power plant in South Africa, finding that our emissions estimate shows reasonable agreement with other independent estimates.

We found that it is feasible to infer CO<sub>2</sub> emissions from satellite NO<sub>2</sub> observations, but limitations of the current satellite data (e.g., spatio-temporal resolution, signal-to-noise) only allow us to apply our method to eight large and isolated U.S. power plants. Looking forward, we anticipate that these limitations will diminish for the recently launched (October 2017) TROPOMI, and three upcoming (launches expected in the early 2020s) geostationary instruments (NASA TEMPO; European Space Agency and Copernicus Programme Sentinel-4; Korea Meteorological Administration Geostationary Environment Monitoring Spectrometer, GEMS), which are designed to have superior capabilities to OMI. As demonstrated in Ialongo et al. (2019), high resolution TROPOMI observations are capable of describing the spatio-temporal variability of NO<sub>2</sub>, even in a relatively small city like Helsinki. Higher spatial and temporal resolutions will likely reduce uncertainties in estimates of NO<sub>x</sub> emissions as well as allow for the separation of more power plant plumes from nearby sources, thus increasing the number of power plants available for analysis. Therefore, future work will be to apply our method to these

new datasets, especially after several years of vetted data become available. Additional future work will include applying our method to other regions of the world with reliable CEMS information, such as Europe, Canada and, more recently, China, to develop a more reliable and complete database with region-specific ratios. ”

*Figure 2: Do the emissions shown in this figure correspond to the ozone season only? If so, this should be indicated in the figure caption. The regression coefficients could be reported only with one or two digits after the point. Is there a reason for showing a linear regression with the intercept term in the panel (c) and without the intercept in other panels?*

**Response:** For comparison to  $E_{NO_x}^{Sat}$  and  $E_{CO_2}^{Sat}$ , we use emissions averaged over the ozone season derived from Air Markets Program Data (available at <https://ampd.epa.gov/ampd/>). However, Air Markets Program Data do not provide information about each plant’s boiler firing types (e.g., tangential or wall-fired boiler), NO<sub>x</sub> control device type, fossil fuel type (with categories of coal, oil, gas and other), and coal type (with categories of bituminous, lignite, subbituminous, refined and waste coal), which are required to get reasonable ratio. Thus, we choose eGRID as the data source for Figure2. We use eGRID annual emissions in Figure 2, because eGRID does not provide CO<sub>2</sub> emissions specifically for the ozone season.

We have changed the regression coefficients to two digits after the point. We intent to show the linear regression without intercept in panels (a) and (b), because the regression slope was calculated requiring zero intercept for deriving  $ratio_{regressed}^{CEMS}$ .

*Figure 8: The meaning of a shaded band should be clearly explained in the figure caption. I suggest also to supply the emission estimates inferred from the OMI observations with the error bars corresponding to the mean of the standard deviations reported in Table 3.*

**Response:** We have added the explanation for the shaded band in the revised caption, as follows: “The upper and lower grey bands denote the emissions inferred from  $ratio_{regressed}^{CEMS}$  and  $ratio_{regressed}^{CEMS} +$  standard deviation of ratio, respectively.”

We have added error bars in the revised figure.

# A methodology to constrain carbon dioxide emissions from coal-fired power plants using satellite observations of co-emitted nitrogen dioxide

Fei Liu<sup>1,2</sup>, Bryan N. Duncan<sup>2</sup>, Nickolay A. Krotkov<sup>2</sup>, Lok N. Lamsal<sup>1,2</sup>, Steffen Beirle<sup>3</sup>, Debora Griffin<sup>4</sup>, Chris A. McLinden<sup>4</sup>, Daniel L. Goldberg<sup>5</sup>, and Zifeng Lu<sup>5</sup>

<sup>1</sup>Universities Space Research Association (USRA), Goddard Earth Sciences Technology and Research (GESTAR), Columbia, MD, USA

<sup>2</sup>Goddard NASA Goddard Space Flight Center, Greenbelt, MD, USA

<sup>3</sup>Max-Planck-Institut für Chemie, Mainz, Germany

<sup>4</sup>Air Quality Research Division, Environment and Climate Change Canada, Toronto, ON, Canada

<sup>5</sup>Energy Systems Division, Argonne National Laboratory, Lemont, IL, USA

Correspondence to: Fei Liu (fei.liu@nasa.gov)

**Abstract.** We present a ~~novel~~ method to infer CO<sub>2</sub> emissions from individual power plants based on satellite observations of co-emitted nitrogen dioxide (NO<sub>2</sub>) ~~and~~, which could serve as complementary verification of bottom-up inventories or be used to supplement these inventories. We demonstrate its utility on eight large and isolated US power plants, where accurate stack emission estimates of both gases are available for comparison. In the first step of our methodology, we infer nitrogen oxides (NO<sub>x</sub>) emissions from isolated US power plants using Ozone Monitoring Instrument (OMI) NO<sub>2</sub> tropospheric vertical column densities (VCDs) averaged over the ozone season (May-September) and a “top-down” approach that we previously developed. Second, we determine the relationship between NO<sub>x</sub> and CO<sub>2</sub> emissions based on the direct stack emissions measurements reported by continuous emissions monitoring system (CEMS) programs, accounting for coal typequality, boiler firing typetechnology, NO<sub>x</sub> emission control device type, and changesany change in operating conditions. Third, we estimate CO<sub>2</sub> emissions ~~of the ozone season~~ for a plantpower plants using the OMI-estimated NO<sub>x</sub> emissions and the CEMS NO<sub>x</sub>/CO<sub>2</sub> emission ratio. We find that the CO<sub>2</sub> emissions estimated by our satellite-based method during 2005–2017 are in reasonable agreement with the US CEMS measurements, with a relative difference of 8% ± 41% (mean ± standard deviation) ~~for the selected US power plants in our analysis. Total uncertainty in the inferred CO<sub>2</sub> estimates is partly associated with the uncertainty associated with the OMI-NO<sub>2</sub> VCD data, so we expect that it will decrease when our method is applied to OMI-like sensors with improved capabilities, such as TROPospheric Monitoring Instrument (TROPOMI) and geostationary Tropospheric Emissions: Monitoring Pollution (TEMPO).~~ The broader implication of our methodology is that it has the potential to provide an additional constraint on CO<sub>2</sub> emissions from power plants in regions of the world without reliable emissions accounting. We explore the feasibility by comparing the derived NO<sub>x</sub>/CO<sub>2</sub> emission ratios for the US with those from a bottom-up emission inventory for other countries and applying our methodology to a power plant in South Africa, where the satellite-based emission estimates show reasonable consistency with other estimatesindependent estimates. Though our analysis is limited to a few power plants, we expect to be able to apply our method to more US (and world) power plants when multi-year data records become available from new OMI-like sensors with improved capabilities, such as the TROPospheric Monitoring Instrument (TROPOMI) and upcoming geostationary satellites, such as the Tropospheric Emissions: Monitoring Pollution (TEMPO) instrument.

## 1 Introduction

Thermal power plants, particularly coal-fired power plants, are among the largest anthropogenic CO<sub>2</sub> emitters, contributing ~40% of energy-related CO<sub>2</sub> emissions globally in 2010 (Janssens-Maenhout et al., 2017). Coal-fired power

1 plants are expected to be one of the primary contributors of CO<sub>2</sub> emissions in the coming decades because of abundant world  
2 coal reserves (Shindell and Faluvegi, 2010). Therefore, it is important to accurately monitor global CO<sub>2</sub> emissions from  
3 power production in order to better predict climate change (Shindell and Faluvegi, 2010) and to support the development of  
4 effective climate mitigation strategies.

5 CO<sub>2</sub> emissions from power plants are typically quantified based on bottom-up approaches using fuel consumption and  
6 fuel quality, though fuel properties are not always well known, resulting in uncertainties in the estimated CO<sub>2</sub> emissions for  
7 individual plants (Wheeler and Ummel, 2008). Even for US power plants that are considered to have the most accurate  
8 information on fuel usage among world nations, the difference between emissions estimated based on fuel usage and those  
9 reported as part of continuous emissions monitoring systems (CEMS) programs is typically about 20% (Ackermann and  
10 Sundquist, 2008). Thus, emission estimates based on independent data sources, such as satellite observations, are a desirable  
11 complement to validate and improve the current CO<sub>2</sub> emissions inventories, especially in countries without CEMS data,  
12 which is the case in most of the world.

13 Anthropogenic CO<sub>2</sub> emissions have been estimated from space-based CO<sub>2</sub> observations, but the existing satellite CO<sub>2</sub>  
14 sensors are designed to provide constraints on natural CO<sub>2</sub> sources and sinks (Basu et al., 2013; Houweling et al, 2015), and  
15 thus their capability for monitoring anthropogenic point sources is limited (Nassar et al., 2017). Observations from sensors,  
16 including the Scanning Imaging Absorption Spectrometer for Atmospheric Chartography (SCIAMACHY; Burrows et al.,  
17 1995), Greenhouse gases Observing SATellite (GOSAT; Yokota et al., 2009), and Orbiting Carbon Observatory-2 (OCO-2;  
18 Crisp et al., 2015), show statistically significant enhancements over metropolitan regions (Kort et al., 2012; Schneising et al.,  
19 2013; Janardanan et al., 2016; Buchwitz et al., 2018; Reuter et al., 2019); [Wang et al., 2018](#)). However, very few studies  
20 have focused on individual point sources. Bovensmann et al. (2010) and Velazco et al. (2011) presented a promising satellite  
21 remote sensing concept to infer CO<sub>2</sub> emissions for power plants based on the atmospheric CO<sub>2</sub> column distribution. Nassar et  
22 al. (2017) ~~and Reuter et al. (2019)~~ presented the [only first](#) quantification of CO<sub>2</sub> emissions from individual power plants using  
23 OCO-2 observations. However, ~~due to~~ [because of](#) the narrow swath ([~10 km at nadir](#)) and [16-day repeat cycle](#) of the OCO-2  
24 sensor, ~~their method cannot be currently applied to generate~~ [the number of clear-day overpasses is too small to allow for the](#)  
25 [development of](#) a global CO<sub>2</sub> emissions database.

26 In contrast to CO<sub>2</sub>, inferring NO<sub>x</sub> emissions from individual power plants using satellite NO<sub>2</sub> column retrievals has been  
27 done with a higher degree of confidence (e.g., Duncan et al., 2013; de Foy et al., 2015). The Dutch-Finnish Ozone  
28 Monitoring Instrument (OMI) on NASA's Earth Observing System Aura spacecraft (Schoeberl et al., 2006) provides [near](#)  
29 daily, global NO<sub>2</sub> tropospheric ~~vertical column densities (VCDs)~~ at a spatial resolution of 13 × 24 km<sup>2</sup> (at nadir) (Levelt et al.,  
30 2006; 2018; Krotkov et al., 2017), which allows emission signals from individual power plants to be resolved. Beirle et al.  
31 (2011) first analyzed isolated large sources (i.e., megacities and the US Four Corners power plant) by averaging OMI NO<sub>2</sub>  
32 tropospheric VCDs separately for different wind directions, which allows ~~to determine~~ [for the estimation of](#) NO<sub>x</sub> emissions  
33 and lifetimes by fitting an exponentially modified Gaussian function. Several follow-up studies (e.g., de Foy et al., 2015; Lu  
34 et al., 2015 and Goldberg et al., 2019a) further developed this approach and inferred NO<sub>x</sub> emissions from isolated power  
35 plants and cities. More recently, we advanced this approach for sources located in polluted areas to infer NO<sub>x</sub> emissions for  
36 17 power plants and 53 cities across China and the US (Liu et al., 2016; 2017).

37 Since NO<sub>x</sub> is co-emitted with CO<sub>2</sub>, NO<sub>x</sub> emissions inferred from satellite data may be used to estimate CO<sub>2</sub> emissions  
38 from thermal power plants. Previous analyses estimated regional CO<sub>2</sub> emissions based on satellite-derived NO<sub>x</sub> emissions  
39 and the NO<sub>x</sub> to CO<sub>2</sub> emission ratios from bottom-up emission inventories (Berezin et al., 2013; Konovalov et al., 2016;  
40 [Goldberg et al., 2019b](#)) or co-located satellite retrievals of CO<sub>2</sub> and NO<sub>2</sub> (Reuter et al., 2014). Hakkarainen et al. (2016)  
41 confirmed the spatial correlation between CO<sub>2</sub> spatial anomalies and OMI NO<sub>2</sub> VCD enhancements at the regional scale  
42 using satellite observations at higher resolution. ~~More recently, the co-located regional enhancements of CO<sub>2</sub> observed by~~

1 ~~OCO-2 and NO<sub>2</sub> observed by TROPOMI were analysed to monitor localized CO<sub>2</sub> emissions (Reuter et al.,~~  
2 ~~2019).~~Hakkarainen et al. (2019) also showed how overlapping OCO-2 CO<sub>2</sub> data and data of NO<sub>2</sub> from the recently launched  
3 (October 2017) European Union Copernicus Sentinel 5 precursor TROPospheric Monitoring Instrument (TROPOMI) can be  
4 used to identify small scale anthropogenic CO<sub>2</sub> signatures.

5 More recently, the co-located regional enhancements of CO<sub>2</sub> observed by OCO-2 and NO<sub>2</sub> observed by TROPOMI were  
6 analysed to infer localized CO<sub>2</sub> emissions for six hotspots including one power plant globally (Reuter et al., 2019). As  
7 emissions plumes are significantly longer than the swath width of OCO-2 (10 km), OCO-2 sees only cross sections of  
8 plumes, which may not be sufficient to infer emission strengths. Because power plant emissions can have substantial  
9 temporal variations (Velazco et al., 2011) and the cross-sectional CO<sub>2</sub> fluxes are valid only for OCO-2 overpass times, the  
10 cross-sectional fluxes may not adequately represent the annual or monthly averages, which are required for the development  
11 of climate mitigation strategies. In addition, the cross-sectional fluxes may not be a good approximation for emission  
12 strengths if meteorological conditions are not taken into account (Varon et al., 2018). As compared to the method proposed  
13 in this study, Reuter's method has the advantage of not requiring a priori emission information. However, there are currently  
14 no satellite instruments with a wide enough swath to allow wider application of Reuter's method.

15 In this study, we present a ~~novel~~ method to estimate CO<sub>2</sub> emissions from individual power plants using OMI NO<sub>2</sub>  
16 observations and auxiliary CEMS information ~~on necessary to estimate~~ NO<sub>x</sub> to CO<sub>2</sub> emission ratios. Such estimates could  
17 serve as complementary verification of bottom-up CO<sub>2</sub> inventories or be used to supplement these inventories. For instance,  
18 Liu et al. (2018) used satellite data of SO<sub>2</sub> to identify large SO<sub>2</sub> sources that were missing from a bottom-up emissions  
19 inventory and created a merged bottom-up/top-down SO<sub>2</sub> emissions inventory. We apply our approach to US power plants,  
20 which have an exceptionally detailed CEMS database of NO<sub>x</sub> and CO<sub>2</sub> emissions, in order to validate our method. Using  
21 auxiliary CEMS information, we explore the relationship between NO<sub>x</sub> and CO<sub>2</sub> emissions for individual power plants,  
22 assessing variations in the ratio associated with coal quality, boiler firing type, NO<sub>x</sub> emission control device technology, and  
23 changes in operating conditions. Understanding the causes of these variations will allow for better informed assumptions  
24 when applying our method to power plants that have no or uncertain information on the factors that affect their emissions  
25 ratios. We discuss the uncertainties and limitations applications of our approach. ~~Finally, we present the application of our~~  
26 ~~method to power plants in South Africa. We discuss other, and the~~ potential applications in conclusion, including to other  
27 NO<sub>2</sub> datasets from new and upcoming satellite instruments, which will improve the utility of our method for inferring CO<sub>2</sub>  
28 emissions from power plants around the world. Finally, we discuss future research directions.

## 29 **2 Method**

30 In this section, we present a ~~novel~~ our method to infer CO<sub>2</sub> emissions ( $E_{CO_2}^{Sat}$ ) from satellite-derived NO<sub>x</sub> emissions ( $E_{NO_x}^{Sat}$ )  
31 for individual coal-fired power plants using the following equation:

$$32 \quad E_{CO_2,y}^{Sat} = \frac{E_{NO_x,y}^{Sat}}{ratio_{i,y}^{CEMS}}, \quad (1)$$

33 where  $i$  represents coal type and  $y$  represents the target year. We demonstrate our method on US power plants since there are  
34 accurate CEMS stack measurements of NO<sub>x</sub> and CO<sub>2</sub> emissions with which to validate  $E_{CO_2}^{Sat}$ . In Section 2.1, we describe  
35 how ~~to~~ we estimate  $E_{NO_x}^{Sat}$  from OMI NO<sub>2</sub> tropospheric VCD observations. In Section 2.2, we discuss how ~~to~~ we estimate the  
36 ratio of NO<sub>x</sub> to CO<sub>2</sub> emissions ( $ratio_y^{CEMS} = E_{NO_x,y}^{CEMS} / E_{CO_2,y}^{CEMS}$ ) from CEMS stack measurements in the US Emissions &  
37 Generation Resource Integrated Database (eGRID; USEPA, 2018). Since post-combustion NO<sub>x</sub> control systems, including  
38 selective noncatalytic reduction (SNCR) and selective catalytic reduction (SCR), change the ~~correlation~~ relationship between

1  $E_{NO_x}^{CEMS}$  and  $E_{CO_2}^{CEMS}$ , we present separate methods to determine  $ratio_y^{CEMS}$  for power plants without and with post-combustion  
2  $NO_x$  control systems in Section 2.2.1 and Section 2.2.2, respectively. We discuss the validation of the estimated  $E_{CO_2}^{Sat}$  in  
3 Section 3.

## 4 2.1 Estimating satellite-derived $NO_x$ emissions ( $E_{NO_x}^{Sat}$ )

5 From all US coal-fired power plants, we selected 21 power plants for estimating  $E_{NO_x}^{Sat}$ . We chose these plants based on the  
6 magnitude of their annual emissions (i.e.,  $E_{NO_x}^{CEMS}$  (i.e., > 10 Gg/yr in 2005) and relative isolation from other large sources and  
7 relative isolation from other large sources to avoid “contamination” of a power plant’s  $NO_x$  plumes by  $NO_x$  from other  
8 sources plume. Power plants located in urban areas (i.e., within a radius of 100 km from a city centerscenter), or clustered in  
9 close proximity (i.e., 50 km) with other large industrial plants arewere excluded by visual inspection using satellite imagery  
10 from Google Earth. TheWe used the top 200 largest US cities (rankranked by 2018 population as estimated by the United  
11 States Census Bureau, available at [https://en.wikipedia.org/wiki/List\\_of\\_United\\_States\\_cities\\_by\\_population](https://en.wikipedia.org/wiki/List_of_United_States_cities_by_population)) are-used to  
12 select power plants. As discussed below, we arewere able to estimate  $E_{NO_x}^{Sat}$  for 8 of the 21 plants. The locations of the 8  
13 plants are shown in Figure S1 and given in Table S1.

14 We followfollowed the method of Liu et al. (2016; 2017) to estimate  $E_{NO_x}^{Sat}$  for 2005 to 2017. In our analysis, we useused  
15 OMI  $NO_2$  tropospheric VCDs from the NASA OMI standard product, version 3.1 (Krotkov et al., 2017) together with  
16 meteorological wind information from the Modern-Era Retrospective Analysis for Research and Applications, version 2  
17 (MERRA-2; Gelaro et al., 2017). We only analyzeanalysed data for the ozone season (May-September), in order to exclude  
18 winter data, which have larger uncertainties and  $NO_x$  lifetimes are longer  $NO_x$  lifetime. As in our previous study (Liu et al.,  
19 2017), we calculated 1-dimensional  $NO_2$  “line densities”, i.e.  $NO_2$  per cm, as function of distance for each wind directions  
20 separately by integration of the mean  $NO_2$  VCDs (i.e.  $NO_2$  per  $cm^2$ ) perpendicular to the wind direction. We thenuse used the  
21 changes of  $NO_2$  line densitiesVCDs under calm wind conditions (wind speed < 2 m/s below 500 m) and windy conditions  
22 (wind speed > 2 m/s) to fit the effective  $NO_x$  lifetime. We then estimateestimated the average  $NO_2$  total mass integrated  
23 around a power plant on the basis of the 3-year mean VCDs, in agreement with previous studies (Fioletov et al., 2011; Lu et  
24 al., 2015). The  $NO_2$  total mass iswas scaled by a factor of 1.32 in order to derive total  $NO_x$  mass following Beirle et al.  
25 (2011). The  $NO/NO_2$  ratio might differ locally in plumes, but the influence is not expected to be dramatic on the scales of  
26 the OMI footprint (at least 13 km×24 km), considering the overpass time of OMI close to noon, the selection of cloud free  
27 observations, and the focus on the ozone season and polluted regions with generally high tropospheric ozone.(2011). The  
28 uncertainty associated with the  $NO/NO_2$  ratio has been discussed in detail in Section 3 of the supplement in Liu et al. (2016).  
29 The 3-year average  $E_{NO_x}^{Sat}$  iswas derived from the corresponding 3-year average  $NO_x$  mass divided by the average  $NO_x$   
30 lifetime of the entire study period (Liu et al., 2017). Fitting results of insufficient quality (e.g., correlation coefficient of the  
31 fitted and observed  $NO_2$  distributions <0.9) arewere excluded from this analysis, consistent with the criteria in Section 2.2 of  
32 Liu et al. (2016). This final filtering leavesleft 18 power plants, of which 8 havehad valid results for all consecutive 3-year  
33 periods between 2005 and 2017. More details of the approach are documented in Liu et al. (2017). The fitted lifetimes and  
34 other fitting parameters for all power plants are given in Table S1.

35 We use the Rockport power plant (37.9°N, 87.0°W) in Indiana to demonstrate our approach. This power plant is  
36 particularly well suited for estimating  $E_{NO_x}^{Sat}$ , because it is a large and isolated  $NO_x$  point source. Figure 42 presents the  $NO_2$   
37 VCD map around Rockport and the fitted results. Figure 3 displays  $E_{NO_x}^{Sat}$  based on 3-year mean VCDs. For simplicity,  
38 theEach 3-year period is represented by the middle year with an asterisk (e.g., 2006\* denotes the period from 2005 to 2007).  
39 For comparison to  $E_{NO_x}^{Sat}$ ,  $E_{NO_x}^{CEMS}$  averaged over the period of May to September is derivedis from Air Markets Program Data  
40 (available at <https://ampd.epa.gov/ampd/>) and averaged over the period of May to September. For this particular plant,

1  $E_{NO_x}^{Sat}$  ~~and is always higher than~~  $E_{NO_x}^{CEMS}$  ~~show positive biases (of varying magnitude)~~ during the entire period, except the last  
2 two years. The coefficient of determination for the entire period is  $R^2=0.68$ . The relative differences for individual 3-year  
3 means (defined as  $(E_{NO_x}^{Sat} - E_{NO_x}^{CEMS})/E_{NO_x}^{CEMS}$ ) range from -20% to 41%, because of the uncertainties of  $E_{NO_x}^{Sat}$  as discussed in  
4 Section 3.2. Both datasets present a declining trend from 2012\*. The total declines of 45% and 26% since 2012\* in  $E_{NO_x}^{Sat}$  and  
5  $E_{NO_x}^{CEMS}$  are attributed to the 25% decrease in net electricity generation for the plant. The average relative difference of  
6  $E_{NO_x}^{Sat}$  and  $E_{NO_x}^{CEMS}$  for the 8 plants in this study is  $0\% \pm 33\%$ , ranging from -58% to 72% for individual 3-year periods (Figure  
7 ~~5~~).

## 8 2.2 Estimating NO<sub>x</sub> to CO<sub>2</sub> emission ratios using CEMS data ( $ratio^{CEMS}$ )

9 We ~~determined~~ ~~the observed~~ relationship between  $E_{NO_x}^{CEMS}$  and  $E_{CO_2}^{CEMS}$  for coal-fired power plants using eGRID  
10 information about each plant's net electric generation, boiler firing ~~type~~ ~~technology~~ (e.g., tangential or wall-fired boiler),  
11 NO<sub>x</sub> control device type, fossil fuel ~~type (with categories of category (i.e., coal, oil, gas and other), and coal type (with~~  
12 ~~categories of quality (i.e., bituminous, lignite, subbituminous, refined and waste coal).~~ We ~~only use~~ ~~used~~ data of power plants  
13 with more than 99% of the fuel burned being coal as reported in eGRID. We ~~analyze~~ ~~analyzed~~ the relationship between  
14  $E_{NO_x}^{CEMS}$  and  $E_{CO_2}^{CEMS}$  by coal type, as emission characteristics vary widely by coal type.

15 eGRID includes two ~~sets~~ ~~datasets~~ of ~~emission data~~ ~~emissions~~ for NO<sub>x</sub> and CO<sub>2</sub>: 1) calculated from fuel consumption data  
16 and 2) observed by stack monitoring (i.e.,  $E_{NO_x}^{CEMS}$  and  $E_{CO_2}^{CEMS}$ ). Here we focus on eGRID CEMS data as  $E_{NO_x}^{CEMS}$  are reported to  
17 be highly accurate with an error of less than 5% (e.g., Glenn et al., 2003).  $E_{CO_2}^{CEMS}$  may have larger uncertainties than fuel-  
18 based emissions estimates ~~due to~~ ~~because of~~ uncertainties in the calculation of flue gas flow (Majanne et al., 2015).  
19 Nevertheless, we ~~use~~ ~~used~~  $E_{CO_2}^{CEMS}$  to relate NO<sub>x</sub> emissions to CO<sub>2</sub> emissions, since the primary uncertainty of  $E_{NO_x}^{CEMS}$  and  $E_{CO_2}^{CEMS}$   
20 arises from the calculation of the flue gas flow, which will cancel in  $ratio^{CEMS}$ .

### 21 2.2.1 Coal-fired power plants without post-combustion NO<sub>x</sub> control systems

22 We ~~first~~ ~~initially~~ limited our analysis to  $E_{NO_x}^{CEMS}$  and  $E_{CO_2}^{CEMS}$  from coal-fired power plants without post-combustion NO<sub>x</sub>  
23 control systems in operation in a given year (Table 1). We find that  $E_{NO_x}^{CEMS}$  and  $E_{CO_2}^{CEMS}$  have a strong linear relationship  
24 (Figure ~~24~~). In Figure ~~2a4a~~, we compare  $E_{NO_x}^{CEMS}$  and  $E_{CO_2}^{CEMS}$  from power plants (using bituminous coal) by boiler firing type in  
25 2005. We use bituminous coal-fired plants for illustration, as bituminous coal is the most widely used coal in US power  
26 plants. We ~~analyze~~ ~~analyzed~~ power plants that use cyclone or cell burner boilers separately and exclude them in Figure ~~24~~  
27 because they typically produce higher NO<sub>x</sub> emissions than other boiler types (USEPA, 2009; available at  
28 <https://www3.epa.gov/ttn/chief/ap42/ch01/index.html>). A strong linear relationship between  $E_{NO_x}^{CEMS}$  and  $E_{CO_2}^{CEMS}$  is evident with  
29 excellent correlation ( $R^2= 0.93$ ,  $N = 278$ ), regardless of boiler firing ~~type~~ ~~type~~. Similar linear relationships exist for other  
30 years (e.g., year 2016 in Figure ~~2b4b~~) and other types of coal (Table 1). The slope of the regression of  $E_{NO_x}^{CEMS}$  and  $E_{CO_2}^{CEMS}$ ,  
31  $ratio_{regressed}^{CEMS}$ , is assumed by setting the intercept to zero. Table 1 shows  $ratio_{regressed,i,y}^{CEMS}$  by coal type and year. ~~In Section~~  
32 ~~3.1,~~  $ratio_{regressed,i,y}^{CEMS}$  will be applied to approximate  $ratio_{i,y}^{CEMS}$  when estimating  $E_{CO_2}^{Sat}$  from  $E_{NO_x}^{Sat}$  for the 8 plants ~~in Section~~  
33 ~~2.4(Figure 1)~~ for years before post-combustion control systems were in operation.

34  $ratio_{regressed}^{CEMS}$  for power plants using bituminous coal decreased from 2005 (Figure ~~2a4a~~) to 2016 (Figure ~~2b4b~~) by 31%  
35 on average because of reductions in NO<sub>x</sub> emission factors associated with improvements in boiler operations, such as by  
36 optimizing furnace design and operating conditions. The NO<sub>x</sub> emissions factors, defined as NO<sub>x</sub> emission rates per net  
37 electricity generation (Gg/TW h), ~~declined~~ by 33% from 2005 to 2016 (Figure ~~2e4c~~). We ~~interpolate~~ ~~interpolated~~

1  $ratio_{regressed}^{CEMS}$  to get year-specific ratios by coal type for the entire study period, as eGRID data are only available for some  
2 years (i.e., 2005, 2007, 2009, 2010, 2012, 2014 and 2016).

3 In addition,  $ratio_{regressed}^{CEMS}$  shows significant variation by coal type and year (Figure 35).  $ratio_{regressed}^{CEMS}$  is 1.7, 1.3 and  
4 0.91 Gg NO<sub>x</sub>/Tg CO<sub>2</sub> for bituminous, subbituminous and lignite coal types in 2005, respectively. A reduction over time in  
5  $ratio_{regressed}^{CEMS}$  is observed for all coal types (Figure 35).  $ratio_{regressed}^{CEMS}$  displays a large decrease of 31%, 36% and 20%  
6 from 2005 to 2016 for bituminous, subbituminous, and lignite coal types, respectively.

## 7 2.2.2 Coal-fired power plants with post-combustion NO<sub>x</sub> control systems

8 Here, we describe how we ~~create continuous and consistent records of estimated~~  $ratio^{CEMS}$  for the entire study period for  
9 plants that had post-combustion NO<sub>x</sub> control systems installed at some time during our study period, 2005–2017. The  
10 estimation is based on  $ratio_{regressed}^{CEMS}$  derived in Section 2.2.1 for plants without post-combustion control systems in  
11 operation. We introduce a NO<sub>x</sub> removal efficiency parameter,  $f$ , to adjust  $ratio_{regressed}^{CEMS}$  for years after the installation of  
12 post-combustion control systems,  $ratio^{CEMS-Estimated}$ :

$$13 \quad ratio_{i,y}^{CEMS-Estimated} = ratio_{regressed,i,y}^{CEMS} \times (1 - f_y), \quad (2)$$

14  $f$  is commonly measured for individual power plants to describe the performance of their post-combustion NO<sub>x</sub> control  
15 systems. It is directly reported by some power plant databases, such as the China coal-fired Power plant Emissions Database  
16 (CPED; Liu et al., 2015). For databases that do not report  $f$ , like eGRID used in this study, one can estimate it for an  
17 individual power plant by first estimating the unabated emissions per electricity generation,  $e_{unabated}$ , which is the emission  
18 factor before the flue gas enters the post-combustion control system:

$$19 \quad f_y = \frac{e_{unabated,y} - e_{CEMS,y}}{e_{unabated,y}}, \quad (3)$$

20 where  $e_{CEMS}$  denotes the actual emission factor in terms of CEMS NO<sub>x</sub> emissions per net electricity generation (Gg/TW h).  
21  $e_{unabated}$  for a given year,  $e_{unabated,y}$  is estimated based on the emission per electricity generation for years prior ~~to~~,  $p$ , to the  
22 installation of the post-combustion control system,  $e_{unabated,p}$ :

$$23 \quad e_{unabated,y} = k_y \times e_{unabated,p}, \quad (4)$$

24 where the scaling factor,  $k_y$ , is used to account for the change over time in  $e_{unabated}$  associated with improvements in boiler  
25 operations discussed in Section 2.2.1.  $k_y$  is calculated as the ratio of the averaged  $e_{unabated}$  (i.e., the slope of the regression of  
26 NO<sub>x</sub> emissions on electricity generation) in year,  $t$ , to that in year,  $p$ .

27 To assess the reliability of  $ratio^{CEMS-Estimated}$ , we ~~selects~~selected all power plants which had post-combustion devices  
28 installed between 2005 and 2016. Figure 46 shows a scatterplot of  $ratio^{CEMS}$  (i.e., the ratio of  $E_{NO_x}^{CEMS}$  to  $E_{CO_2}^{CEMS}$  for individual  
29 plantplants) and  $ratio^{CEMS-Estimated}$  ~~for these power plants.~~ We used the NO<sub>x</sub> emissions factor in 2005,  $e_{unabated,2005}$ , to  
30 predict the unabated emission factor in 2016,  $e_{unabated,2016}$ , following Equations (3) and (4) in order to quantify the removal  
31 efficiencies for 2016,  $f_{2016}$ .  $ratio_{2016}^{CEMS-Estimated}$  is based on the estimated  $f_{2016}$  and  $ratio_{regressed,2016}^{CEMS}$  from Section 2.2.1.  
32  $ratio^{CEMS}$  and  $ratio^{CEMS-Estimated}$  show good correlation ( $R^2 = 0.64$ ), which increases our confidence that the estimated  
33 removal efficiencies approximate the actual efficiencies ~~well~~. The slight underestimation suggested by the slope of 0.85  
34 arises from ~~the~~ uncertainties in estimating unabated NO<sub>x</sub> emission factors ( $e_{unabated,y}$ ) using Equation (4) and thus removal  
35 efficiencies, ( $f$ ), which is a major source of error of  $E_{CO_2}^{Sat}$  for power plants that install post-combustion NO<sub>x</sub> control systems  
36 (see details in Section 3.2) ~~contributing to the overall uncertainties of  $E_{CO_2}^{Sat}$ .~~



### 3 Results and Discussion

In Section 3.1, we present  $E_{CO_2}^{Sat}$  for our eight selected power plants and, in Section 3.2, we discuss the uncertainties associated with  $E_{CO_2}^{Sat}$ . We In Section 3.3, we compare the US ratios derived in this study with those from a bottom-up inventory for other regions to explore the potential of applying our method to regions outside the US. We finally apply theour approach to one power plantsplant in South Africa, which has several independent estimates for its CO<sub>2</sub> emissions as presented in the scientific literature. Table 2 shows three-year means of  $E_{NO_2}^{Sat}$ ,  $E_{NO_2}^{CEMS}$ ,  $E_{CO_2}^{Sat}$  and  $E_{CO_2}^{CEMS}$  for eight power plants (Figure 1). Table 3 lists the mean and the standard deviation of the relative differences between  $E_{NO_x}^{CEMS}$  and  $E_{NO_x}^{Sat}$ , and  $E_{CO_2}^{CEMS}$  and  $E_{CO_2}^{Sat}$  for all eight power plants.

#### 3.1 Satellite-derived CO<sub>2</sub> emissions ( $E_{CO_2}^{Sat}$ )

Figure 6a7a is a scatterplot of  $E_{CO_2}^{Sat}$  and  $E_{CO_2}^{CEMS}$  for the eight power plants (Figure 5), seven of which did not have post-combustion NO<sub>x</sub> control systems installed during the study period, 2005–2017. The comparison shows a good correlation,  $R^2$ , of 0.66.  $E_{CO_2}^{Sat}$  and  $E_{CO_2}^{CEMS}$  for individual power plants are tabulated in Table 2 and their relative difference with CEMS measurements are listed in Table 3. The average  $E_{CO_2}^{CEMS}$  for all power plants is 2.0 Gg/h and the average  $E_{CO_2}^{Sat}$  is 1.8 Gg/h. The relative difference for individual three year means (defined as  $(E_{CO_2}^{Sat} - E_{CO_2}^{CEMS})/E_{CO_2}^{CEMS}$ ) is  $8\% \pm 41\%$  (mean  $\pm$  standard deviation). For example, Figure 13 shows  $E_{CO_2}^{Sat}$  for the Rockport power plant, which typically has a positive bias as compared to  $E_{CO_2}^{CEMS}$  because of a positive bias in  $E_{NO_x}^{Sat}$ . The average  $E_{CO_2}^{CEMS}$  for all power plants is 2.0 Gg/h and the average  $E_{CO_2}^{Sat}$  is 1.8 Gg/h. The relative difference for individual three year means (defined as  $(E_{CO_2}^{Sat} - E_{CO_2}^{CEMS})/E_{CO_2}^{CEMS}$ ) is  $8\% \pm 41\%$  (mean  $\pm$  standard deviation). For example, Figure 3 shows  $E_{CO_2}^{Sat}$  for the Rockport power plant, which typically has a positive bias as compared to  $E_{CO_2}^{CEMS}$  because of a positive bias in  $E_{NO_x}^{Sat}$ .

The time series between  $E_{CO_2}^{Sat}$  and  $E_{CO_2}^{CEMS}$  are generally consistent, with their annual averages for the eight power plants exhibiting a declining trend of 5%/yr and 3%/yr from 2006\* to 2016\* for  $E_{CO_2}^{Sat}$  and  $E_{CO_2}^{CEMS}$ , respectively. The reduction in net electricity generation is the driving force underlying the emission changes, which has decreased by 37% for the eight power plants from 2005 to 2016, as power producers shut down coal-fired units in favor of cheaper and more flexible natural gas as well as solar and wind (USEIA, 2018). It is interesting to note that the temporal variations in  $E_{CO_2}^{Sat}$  are not as “smooth” as those in  $E_{CO_2}^{CEMS}$ , which results from fluctuations in  $E_{NO_x}^{Sat}$ . Such fluctuations are caused by uncertainties associated with  $E_{NO_x}^{Sat}$  as discussed in Section 3.2. For example, changes in VCDs do not necessarily relate linearly with NO<sub>x</sub> emissions (e.g., Figure 2 in Duncan et al., 2013) due tobecause of temporal variations in meteorology, and nonlinear NO<sub>x</sub> chemistry (Valin et al, 2013) and transport. Averaging VCDs for a long-term period (3 years in this study) helps reduce those influences, but small fluctuations may still exist.

#### 3.2 Uncertainties

We estimateestimated the uncertainty of  $E_{CO_2}^{Sat}$  based on the fit performance of  $E_{NO_x}^{Sat}$  and comparison with  $E_{CO_2}^{CEMS}$ . The major sources of uncertainty include (a) the fitted NO<sub>x</sub> lifetimes and are (a)  $E_{NO_x}^{Sat}$  (Liu et al., 2016); (b)  $ratio_{regressed}^{CEMS}$ ; and (c)  $f$ . We assume that their contributions to the total uncertainty are independent and define the total uncertainty as their root mean squareWe give the estimated uncertainties of each source for individual power plants in Table S2.

(a) The uncertainty of the fitted NO<sub>x</sub> lifetimes and  $E_{NO_x}^{Sat}$  are . The uncertainty of  $E_{NO_x}^{Sat}$  is quantified following the method described in Liu et al. (2017), accounting for errors arising from boththe fit procedure, the NO<sub>x</sub>/NO<sub>2</sub> ratio and OMI NO<sub>2</sub> VCD observations (Liu et al., 2016). ParticularlyThe number of 1.32 used for scaling the NO<sub>2</sub> to NO<sub>x</sub> ratio is based on assumptions presented in section 6.5.1 of Seinfeld and Pandis (2006) for “typical urban conditions and noontime sun”. Note

1 that conditions are quite similar in this study because of the overpass time of OMI close to noon, the selection of cloud-free  
2 observations, the focus on the ozone season, and the focus on polluted regions. A case study of CTM simulations shows an  
3 identical value of 1.32 for Paris in summer (Shaiganfar et al., 2017). The simulated  $\text{NO}_x/\text{NO}_2$  ratio at the OMI overpass time  
4 within the boundary layer (up to 2 km) in a chemistry–climate model, EMAC (Jöckel et al., 2016), was  $1.28 \pm 0.08$  for  
5 polluted ( $\text{NO}_x > 1 \times 10^{15}$  molec  $\text{cm}^{-2}$ ) regions for the July 1, 2005, and  $1.32 \pm 0.06$  on average for the ozone season. However,  
6 the coarse grid of EMAC ( $2.8^\circ \times 2.8^\circ$  in latitude and longitude) may not capture the true range of variation of the  $\text{NO}_x/\text{NO}_2$   
7 ratio. Therefore, we assumed an uncertainty of 20% arising from the  $\text{NO}_x/\text{NO}_2$  ratio, double than the standard deviation of  
8 the EMAC ratio.

9 Additionally, the tropospheric air mass factors (AMF) used in  $\text{NO}_2$  retrievals are based on relatively coarsely–resolved  
10 surface albedo data and a priori  $\text{NO}_2$  vertical profile shapes, likely causing low-biased VCDs over strong emission sources  
11 (e.g., Russell et al., 2011; McLinden et al., 2014; Griffin et al., 2019). The average AMF uncertainty of ~30% (see Table 2 in  
12 Boersma et al., 2007) likely contributes to the underestimation of emissions from some power plants in this study. Both  
13 random and systematic (bias) uncertainties in VCDs directly propagates into the uncertainty of  $E_{\text{NO}_x}^{\text{Sat}}$  (see details in the  
14 supplement of Liu et al. (2016) and Section 3.4 of Liu et al. (2017)).

15 The overall uncertainties of  $E_{\text{NO}_x}^{\text{Sat}}$  range from ~~60~~57% to ~~95~~64% for all power plants in our analysis, which is comparable  
16 with the level of differences between  $E_{\text{NO}_x}^{\text{Sat}}$  and  $E_{\text{NO}_x}^{\text{CEMS}}$ . We expect this uncertainty to be less for new (e.g., TROPOMI) and  
17 upcoming (e.g., NASA Tropospheric Emissions: Monitoring Pollution, TEMPO) OMI-like sensors, which have enhanced  
18 capabilities relative to OMI. Further details are provided in Text S1 of the Supplement.

19 ~~(b)~~ratio<sub>regressed</sub><sup>CEMS</sup>: For power plants without post-combustion devices, ratio<sub>regressed</sub><sup>CEMS</sup> derived from the regression (Figure  
20 ~~2a4a~~ & b) and the plant-specific CEMS measurements are ~~found to be~~ within 15%, which is assumed as the uncertainty of  
21 the ratio ~~to be applied to~~ for all power plants.

22 ~~(c)~~f: For power plants with post-combustion devices, an additional uncertainty of 20% is applied to reflect the difference  
23 between the predicted and the true removal efficiency as suggested by Figure 46.

24 We assume that their contributions to the overall uncertainty are independent. We then define the total uncertainty,  
25 expressed as a 95% confidence interval, as the sum of the root of the quadratic sum of the aforementioned contribution. The  
26 overall uncertainties of  $E_{\text{CO}_2}^{\text{Sat}}$  ~~range from 62%–96~~are ~60% for ~~the all~~ power plants in our analysis.

27 However, it is worth noting that this uncertainty estimate is rather conservative. ~~For power plants,~~The mean and the  
28 standard deviation of the relative differences between  $E_{\text{NO}_x}^{\text{CEMS}}$  and  $E_{\text{NO}_x}^{\text{Sat}}$ , and  $E_{\text{CO}_2}^{\text{CEMS}}$  and  $E_{\text{CO}_2}^{\text{Sat}}$  ~~are for all eight power~~  
29 plants provide a good alternative measure of uncertainties (Table 3). The relative differences are rather small, which are 0%  
30  $\pm 33\%$  and  $8\% \pm 41\%$  (mean  $\pm$  standard deviation) (Figure 6a) for  $\text{NO}_x$  and  $\text{CO}_2$ , respectively. We additionally calculate the  
31 geometric standard deviations (GSDs) of the difference between  $E_{\text{CO}_2}^{\text{CEMS}}$  and  $E_{\text{CO}_2}^{\text{Sat}}$  from 2006\* to 2016\* for individual power  
32 plants in Table S2. The small values of GSDs ranging from 1.07 to 1.31 further improve our confidence in the accuracy of  
33 the derived emissions in this study.

### 34 **3.3 Application**

35 We apply the approach proposed in this study to estimate  $\text{CO}_2$ -emissions from a power plant in South Africa, aiming to In  
36 this section, we assess the ~~capability~~feasibility of the approach applying our method to provide constraint on infer  $\text{CO}_2$   
37 emissions ( $E_{\text{CO}_2}^{\text{Sat}}$ ) for ~~regions~~power plants outside the US. We chose South Africa, a country without reliable emissions  
38 accounting, as We first compare the  $\text{NO}_x$  to  $\text{CO}_2$  emission ratios derived from this study with those from a bottom-up  
39 emission database in Section 3.3.1. We then apply the US ratio to a power plant in South Africa in Section 3.3.2.

### 3.3.1 Comparison with bottom-up ratios

Figure 8 shows the area of interest, because we found  $\text{NO}_x$  to  $\text{CO}_2$  emission ratios for 2010 from the global power emissions database (GPED; Tong et al., 2018), which is the only publicly-available information on coal-type bottom-up emission database that reports both  $\text{NO}_x$  and  $\text{CO}_2$  emissions for individual power plants for every country. All countries with over 30 coal-fired power plants in GPED are shown in Figure 8. Not surprisingly, countries with more strict standards in place for  $\text{NO}_x$  emissions from power plants (i.e.,  $\text{NO}_x$  emission limit value (ELV)  $< 200 \text{ mg/m}^3$ ; hereafter referred to as “more strict countries”) have smaller  $\text{NO}_x$  to  $\text{CO}_2$  ratios (i.e., 1.0 versus 2.5 on average) than countries with less strict standard (i.e.,  $\text{NO}_x$  ELV  $> 200 \text{ mg/m}^3$ ; hereafter referred to as “less strict countries”). Additionally, the correlation coefficients are smaller for more strict countries (i.e., 0.82 on average) as compared to less strict countries (i.e., 0.96 on average), because power plants in more strict countries are more likely to have installed post-combustion  $\text{NO}_x$  control status for its power plants systems, which likely lowered  $\text{ratio}_y^{\text{CEMS}}$ , similar to what occurred in the US over our analysis period (Section 2.2.2).

We further compare the 2005 US  $\text{ratio}_{regressed}^{\text{CEMS}}$  in Table 1 with the GPED  $\text{NO}_x$  to  $\text{CO}_2$  emission ratios for less strict countries. We chose the 2005 value for comparison based on the following considerations. In 2005, the US EPA issued the Clean Air Interstate Rule (CAIR) to address the interstate transport of ozone and fine particulate matter pollution for eastern US states, which reduced  $\text{NO}_x$  emissions and, thus,  $\text{NO}_x$  to  $\text{CO}_2$  ratios ( $\text{ratio}_y^{\text{CEMS}}$ ). However, similar comprehensive control strategies have not been adopted in less strict countries. In this way, the 2005 values are expected to show better consistency with the  $\text{NO}_x$  to  $\text{CO}_2$  ratios of less strict countries than values for more recent years. Note that the GPED database does not give information on ratios by coal type. Therefore, we use  $\text{ratio}_{regressed}^{\text{CEMS}}$  for bituminous coal, which is the most widely used coal type in coal-fired power plants in most countries.

The power plant of Matimba (including the nearby Medupi) ratios for individual power plants in less strict countries tend to be larger than the US  $\text{ratio}_{regressed}^{\text{CEMS}}$  for 2005, considering that power plants in those countries may not be equipped with any  $\text{NO}_x$  control devices or even low- $\text{NO}_x$  burners, a technology which is widely installed in US power plants with and without post-combustion  $\text{NO}_x$  control devices. Most ratios range from US 2005  $\text{ratio}_{regressed}^{\text{CEMS}}$  to  $\text{ratio}_{regressed}^{\text{CEMS}} + \text{standard deviation}$  (Figure 8). It is no surprise that some less strict countries have ratios higher than this range, which also occurs for some US power plants without post-combustion emission controls (Figure 4). However, there are considerable uncertainties in the GPED database given the scarcity of reliable emissions information in less strict countries. For example, the GPED  $\text{NO}_x$  and  $\text{CO}_2$  emissions estimates for Turkey and Russia, which are outliers in Figure 8, are subject to more assumptions and, thus, larger uncertainties than countries with high-quality country-specific emission data, such as China, which has operated since a high-resolution emissions database (CPED; Liu et al., 2015) in South Africa are, and India, which has a database developed by Argonne National Laboratory (Lu et al., 2011).

Figure 9 shows a schematic of our methodology to estimate the  $\text{NO}_x$  to  $\text{CO}_2$  emission ratios for power plants outside the US. We adopt different approaches for more and less strict countries. More strict countries, including Canada, European Union (EU) member states, Japan, South Korea, and, more recently, China, usually use CEMS to monitor emissions, particularly suitable for application of our method, because from the largest emitters. For power plants with CEMS measurements for both  $\text{NO}_x$  and  $\text{CO}_2$  emissions, it is straightforward to use the measured ratios. However, there is still a significant number of power plants in those countries without CEMS technology, particularly for  $\text{CO}_2$  measurements. For example, EU member states do not require power plants to use CEMS for  $\text{CO}_2$  reporting and the majority of plants in the EU therefore reports  $\text{CO}_2$  emissions based on emission factors (Sloss, 2011). Therefore, we recommend applying our method described in Section 2.2 to infer region-specific ratios for those power plants. The US  $\text{ratio}_{regressed}^{\text{CEMS}}$  could be a less accurate, but reasonable approximation when no CEMS data are available, considering those countries share similar  $\text{NO}_x$  ELVs for power plants as the US. For less strict countries, we recommend using the 2005 US values by coal type when ratios from

1 countries with similar NO<sub>x</sub> emission standard are not available. We also recommend assigning a range from 2005  
2  $ratio_{regressed}^{CEMS}$  to 2005  $ratio_{regressed}^{CEMS}$  + standard deviation, instead of a fixed value, to the ratio for inferring CO<sub>2</sub> emissions,  
3 considering the knowledge on ratios from those regions are too few to narrow the constraint.

4 As demonstrated in Section 2.2, our method presented in this study provides a reasonable estimate of the ratio for power  
5 plants without post-combustion NO<sub>x</sub> control devices with only knowing coal type. Even for regions without reliable  
6 emission information, the information on coal type, particularly for large power plants, are very likely publicly-available. For  
7 power plants that install post-combustion NO<sub>x</sub> control technology, we additionally require the removal efficiency of the  
8 device to derive the ratio. The removal efficiency of post-combustion NO<sub>x</sub> control devices is usually directly reported, as the  
9 operation of such devices is very expensive and is expected to be subject to strict quality control and assurance standards. In  
10 contrast to bottom-up approaches, many details are required, including coal type, coal quality, boiler firing type, NO<sub>x</sub>  
11 emission control device type, and operating condition of boiler and emission control device, when calculating NO<sub>x</sub> and CO<sub>2</sub>  
12 emissions.

### 13 3.3.2 Application to Matimba power plant in South Africa

14 We apply the methodology shown in Figure 9 to estimate CO<sub>2</sub> emissions from a South African power plant, Matimba,  
15 which is a strong isolated NO<sub>x</sub> point source (Figure 7-10). It is a well-studied power plant, having had its emissions  
16 estimated using several different methods as reported in the literature. We estimate  $E_{NO_x}^{Sat}$  for Matimba from 2005 to 2017  
17 based on OMI NO<sub>2</sub> observations following the approach in Section 2.1. Matimba ~~uses~~ subbituminous coal with ~~the~~  
18 calorific value of ~ 20 MJ/kg (Makgato and Chirwa, 2017). ~~We assume the NO<sub>x</sub> to CO<sub>2</sub> emission ratio of Matimba is on the~~  
19 ~~upper end of the US values, considering that it is not equipped with any NO<sub>x</sub> control devices, even low NO<sub>x</sub> burners which~~  
20 ~~are widely installed in US power plants. We apply (Pretorius et al., 2015). We thus use~~ the ratio ranging from 2005  
21  $ratio_{regressed}^{CEMS}$  to 2005  $ratio_{regressed}^{CEMS}$  + standard deviation ~~to Matimba, following the methodology in Figure 9, considering~~  
22 ~~that South Africa is a less strict country without any post-combustion NO<sub>x</sub> control devices (Pretorius et al., 2015). for~~  
23 ~~subbituminous coal listed in Table 1 to infer  $E_{CO_2}^{Sat}$  based on  $E_{NO_x}^{Sat}$ . The Our derived  $E_{CO_2}^{Sat}$  is shown in Figure 8 11 and fluctuates~~  
24 ~~over time. Note that the range of  $E_{CO_2}^{Sat}$  in Figure 8 represents the emissions based on a range of NO<sub>x</sub> to CO<sub>2</sub> ratios, not the~~  
25 ~~uncertainty. The overall uncertainty of  $E_{CO_2}^{Sat}$  is ~70% for the Matimba power plant. The growth after 2008\* is most likely~~  
26 ~~caused by the increased unit operating hours driven by the desire to meet fully the demand for electricity in South Africa~~  
27 ~~after a period of rolling blackouts (2007–2008) (Duncan et al., 2016). The decline afterwards may be associated with the~~  
28 ~~tripping of generating units at the Matimba due to overload and the shortage of coal supply. The newly built power plant of~~  
29 ~~Medupi contributes to the increase from 2015\* because of overload and shortage of coal as reported by South African~~  
30 ~~government news agency (available at [https://www.sanews.gov.za/south-africa/eskom-alone-cannot-solve-our-energy-](https://www.sanews.gov.za/south-africa/eskom-alone-cannot-solve-our-energy-challenges)~~  
31 ~~challenges). The increase in 2016\* may be associated with a newly-built power plant, Medupi, which began limited~~  
32 ~~operations in 2015. Note that the range of  $E_{CO_2}^{Sat}$  (grey band) in Figure 11 represents the emissions based on a range of NO<sub>x</sub>-~~  
33 ~~to-CO<sub>2</sub> ratios, not the uncertainty. We calculate the uncertainty of  $E_{CO_2}^{Sat}$  for Matimba following Section 3.2 with an additional~~  
34 ~~uncertainty of ~50% to reflect the fact that the ratio may range from  $ratio_{regressed}^{CEMS}$  to  $ratio_{regressed}^{CEMS}$  + standard deviation.~~  
35 ~~The overall uncertainty of  $E_{CO_2}^{Sat}$  for Matimba is 81%, as shown by the error bars in Figure 11.~~

36 Figure 8 ~~compares~~ 11 shows  $E_{CO_2}^{Sat}$  derived in this study ~~with~~ and other ~~publicly available~~ independent estimates ~~and shows~~  
37 ~~reasonable agreement. reported in  $E_{CO_2}^{Sat}$  falls between the estimates based on OCO-2 CO<sub>2</sub> observations literature, including~~  
38 ~~two top-down (Nassar et al., 2017; Reuter et al., 2019) and two three bottom-up estimates including (Wheeler and Ummel (,~~  
39 ~~2008) and Tong et al. (, 2018). We make a further comparison; Oda et al., 2018). Despite the uncertainties associated with~~  
40 ~~each of NO<sub>x</sub> these methods, the CO<sub>2</sub> emissions estimates estimates agree reasonably well, but we do not have sufficient~~  
41 ~~information to understand the differences between these estimates. However, Tong et al. (2018), the only) present in their~~

1 ~~CPED~~ database ~~that reports~~ both CO<sub>2</sub> and NO<sub>x</sub> emissions, ~~in order~~ which allows us to ~~shed light on the reason for~~ determine  
2 ~~that~~ the difference. ~~The differences~~ between  $E_{NO_x}^{Sat}$  and ~~the CPED~~ bottom-up ~~estimates~~ ~~contribute~~ ~~estimate~~ ~~contributes~~  
3 significantly to the ~~differences of~~ ~~difference in~~ CO<sub>2</sub> estimates ~~from the two methods~~.  $E_{NO_x}^{Sat}$  for Matimba is 3.8 Mg/h for 2010\*,  
4 which is 65% smaller than the estimate by Tong et al. (2018) for 2010. It is not surprising to see such differences considering  
5 the uncertainties of satellite-derived NO<sub>x</sub> emissions and bottom-up estimates ~~for power plants~~ without reliable CEMS  
6 measurements. ~~On one hand~~ ~~For instance~~,  $E_{NO_x}^{Sat}$  is potentially underestimated, ~~due to~~ ~~because of~~ the bias in the OMI NO<sub>2</sub>  
7 standard product (version 3.1) associated with a low-resolution static climatology of surface Lambert-Equivalent Reflectivity  
8 (OMLER) (Kleipool et al., 2008). We perform a sensitivity analysis by using the preliminary new version ~~of the~~ OMI NO<sub>2</sub>  
9 product, which uses new geometry dependent ~~Moderate Resolution Imaging Spectroradiometer (MODIS-)~~ based surface  
10 reflectivity. The inferred  $E_{NO_x}^{Sat}$  based on the new product ~~increases by~~ ~~is~~ over 10%. ~~On the other hand, the~~ ~~% higher than~~  
11 ~~version 3.1. The~~ bottom-up estimates for Matimba are subject to significant uncertainties ~~as well~~. For example, ~~Tong et al.~~  
12 ~~(2018) used~~ national total fuel consumption of the power sector for South Africa as reported by the International Energy  
13 Agency ~~is used~~ to estimate fuel consumption at the plant level as detailed fuel consumption for each plant is not currently  
14 available. Additionally, ~~due to the absence of country specific measurement data,~~ ~~they used~~ default NO<sub>x</sub> emission factors  
15 obtained from ~~the~~ literature ~~are applied (Tong et al., 2018),~~ ~~because of the absence of country-specific measurement data.~~

## 16 4 Conclusions

17 ~~We present a method to estimate CO<sub>2</sub> emissions of ozone season from individual power plants from satellite observations~~  
18 ~~of co-emitted~~ In our study, we investigated the feasibility of using satellite data of NO<sub>2</sub> from power plants to infer co-emitted  
19 CO<sub>2</sub> emissions, which could serve as complementary verification of bottom-up inventories or be used to supplement these  
20 inventories that are highly uncertain in many regions of the world. For example, our estimates will serve as an independent  
21 check of CO<sub>2</sub> emissions that will be inferred from satellite retrievals of future CO<sub>2</sub> sensors (Bovensmann et al., 2010).  
22 ~~Currently, uncertainties in CO<sub>2</sub> emissions from power plants confound national and international efforts to design effective~~  
23 ~~climate mitigation strategies.~~

24 ~~We estimate NO<sub>2</sub> and CO<sub>2</sub> emissions during the “ozone season” from individual power plants from satellite observations~~  
25 ~~of~~ NO<sub>2</sub> and demonstrate its utility for US power plants, which have accurate CEMS with which to evaluate our method.  
26 ~~While~~ ~~We systematically identify~~ the ~~uncertainty associated with~~ sources of variation, such as types of coal, boiler, and NO<sub>x</sub>  
27 emission control device, and change in operating conditions, which affect the NO<sub>x</sub> to CO<sub>2</sub> emissions ratio. Understanding the  
28 causes of these variations will allow for better informed assumptions when applying our method ~~to power plants that have no~~  
29 ~~or uncertain information on the factors that affect their emissions ratios.~~ For example, we estimated CO<sub>2</sub> emissions from the  
30 large and isolated Matimba power plant in South Africa, finding that our emissions estimate shows reasonable agreement  
31 ~~with other independent estimates.~~

32 ~~We found that it is relatively high when applied to OMI~~ feasible to infer CO<sub>2</sub> emissions from satellite NO<sub>2</sub> observations, but  
33 ~~limitations of the current satellite data,~~ ~~we expect that the uncertainty will be less (e.g., spatio-temporal resolution, signal-to-~~  
34 ~~noise) only allow us to apply our method to eight large and isolated U.S. power plants. Looking forward, we anticipate that~~  
35 ~~these limitations will diminish~~ for the recently launched ~~European Union Copernicus Sentinel 5 precursor (TROPOMI,~~  
36 ~~launch (October 2017),)~~ TROPOMI, and ~~the three~~ upcoming NASA geostationary Earth Venture one (TEMPO,  
37 ~~launch (launches~~ expected in the early 2020s), ~~both of which~~) geostationary instruments (NASA TEMPO; European Space  
38 Agency and Copernicus Programme Sentinel-4; Korea Meteorological Administration Geostationary Environment  
39 ~~Monitoring Spectrometer, GEMS), which are designed to~~ have superior capabilities. ~~For example, higher spatiotemporal to~~  
40 ~~OMI. High resolution TROPOMI observations are capable of describing the spatio-temporal variability of NO<sub>2</sub>, even in a~~

1 ~~relatively small city like Helsinki- (Ialongo et al., 2019) and allow estimates of NO<sub>x</sub> emissions to be calculated for shorter~~  
2 ~~timeframes (Goldberg et al., 2019c). Higher spatial and temporal~~ resolutions will likely ~~improve the estimation~~  
3 ~~uncertainties in estimates~~ of NO<sub>x</sub> emissions as well as allow for the separation of more power plant plumes from nearby  
4 sources, thus increasing the number of power plants available for analysis. Therefore, future work will be to apply our  
5 method to these new datasets, especially after several years of vetted ~~TROPOMI~~ data become available.

6 ~~We explore the feasibility of estimating CO<sub>2</sub> emissions from power plants in regions of the world without reliable~~  
7 ~~emissions accounting by applying our method to a South African plant. The emissions estimates for the power plant of~~  
8 ~~Matimba show reasonable agreement with existing estimates. The ratios derived in this study have the potential to be applied~~  
9 ~~to power plants located in other regions by carefully investigating their coal type and NO<sub>x</sub> control devices, in order to~~  
10 ~~provide an additional constraint on CO<sub>2</sub> emissions. Future~~ Additional future work will include applying our method to other  
11 regions of the world with reliable CEMS information, such as Europe, Canada and, more recently, China, to develop a more  
12 reliable and complete database with region-specific ratios. ~~This method will also serve as an independent approach to check~~  
13 ~~CO<sub>2</sub> emissions based on satellite retrievals of CO<sub>2</sub> average mixing ratio from future CO<sub>2</sub> sensors with improved accuracy~~  
14 ~~and extended the spatial coverage (Bovensmann et al., 2010).~~

### 15 Data availability

16 The OMI NO<sub>2</sub> and MERRA-2 data can be downloaded from the Goddard Earth Sciences Data and Information Services  
17 Center (GES DISC; available at <https://disc.gsfc.nasa.gov/datasets>).

### 18 **Author contribution**

19 Fei Liu, Bryan N. Duncan, and Nickolay A. Krotkov designed the framework. Fei Liu, Steffen Beirle, Lok N. Lamsal,  
20 Debora Griffin, Chris A. McLinden, and Daniel L. Goldberg developed the NO<sub>x</sub> emission fitting algorithm and Fei Liu  
21 carried it out. Fei Liu and Zifeng Lu analysed the NO<sub>x</sub>/CO<sub>2</sub> emission ratio. Fei Liu and Bryan N. Duncan prepared the  
22 manuscript with contributions from all co-authors.

### 24 Competing interests

25 The authors declare that they have no conflict of interest.

### 26 **Acknowledgments**

27 This research has been funded by the NASA's Earth Science Division Atmospheric Composition: Modeling and Analysis  
28 Program (ACMAP) and the Aura Science team. The Dutch-Finnish-built OMI instrument is part of the NASA EOS Aura  
29 satellite payload. KNMI and the Netherlands Space Agency (NSO) manage the OMI project. We thank the US EPA for  
30 making the Emissions & Generation Resource Integrated Database (eGRID) available on line.

### 31 **References**

32 Ackerman, K. V., and Sundquist, E. T.: Comparison of two U.S. power-plant carbon dioxide emissions data sets, Environ.  
33 Sci. Technol., 42, 5688–5693, doi: 10.1021/es800221q, 2008.  
34 Basu, S., Guerlet, S., Butz, A., Houweling, S., Hasekamp, O., Aben, I., Krummel, P., Steele, P., Langenfelds, R., Torn, M.,  
35 Biraud, S., Stephens, B., Andrews, A., and Worthy, D.: Global CO<sub>2</sub> fluxes estimated from GOSAT retrievals of total column  
36 CO<sub>2</sub>, Atmos. Chem. Phys., 13, 8695–8717, doi: 10.5194/acp-13-8695-2013, 2013.

1 Beirle, S., Boersma, K. F., Platt, U., Lawrence, M. G., and Wagner, T.: Megacity emissions and lifetimes of nitrogen oxides  
2 probed from space, *Science*, 333, 1737–1739, 2011.

3 Berezin, E. V., Konovalov, I. B., Ciais, P., Richter, A., Tao, S., Janssens-Maenhout, G., Beekmann, M., and Schulze, E. D.:  
4 Multiannual changes of CO<sub>2</sub> emissions in China: indirect estimates derived from satellite measurements of tropospheric NO<sub>2</sub>  
5 columns, *Atmos. Chem. Phys.*, 13, 9415–9438, doi: 10.5194/acp-13-9415-2013, 2013.

6 Boersma, K. F., Eskes, H. J., Dirksen, R. J., van der A, R. J., Veefkind, J. P., Stammes, P., Huijnen, V., Kleipool, Q. L.,  
7 Sneep, M., Claas, J., Leitão, J., Richter, A., Zhou, Y., and Brunner, D.: An improved tropospheric NO<sub>2</sub> column retrieval  
8 algorithm for the Ozone Monitoring Instrument, *Atmos. Meas. Tech.*, 4, 1905–1928, doi:10.5194/amt-4-1905-2011, 2011.

9 Bovensmann, H., Buchwitz, M., Burrows, J. P., Reuter, M., Krings, T., Gerilowski, K., Schneising, O., Heymann, J.,  
10 Tretner, A., and Erzinger, J.: A remote sensing technique for global monitoring of power plant CO<sub>2</sub> emissions from space  
11 and related applications, *Atmos. Meas. Tech.*, 3, 781–811, doi: 10.5194/amt-3-781-2010, 2010.

12 Buchwitz, M., Reuter, M., Schneising, O., Noth, S., Gier, B., Bovensmann, H., Burrows, J. P., Boesch, H., Anand, J., Parker,  
13 R. J., Somkuti, P., Detmers, R. G., Hasekamp, O. P., Aben, I., Butz, A., Kuze, A., Suto, H., Yoshida, Y., Crisp, D., and  
14 O'Dell, C.: Computation and analysis of atmospheric carbon dioxide annual mean growth rates from satellite observations  
15 during 2003–2016, *Atmos. Chem. Phys.*, 18, 17355–17370, doi: 10.5194/acp-18-17355-2018, 2018.

16 Burrows, J. P., Hölzle, E., Goede, A. P. H., Visser, H., and Fricke, W.: SCIAMACHY—scanning imaging absorption  
17 spectrometer for atmospheric cartography, *Acta Astronaut.*, 35, 445–451, doi: [https://doi.org/10.1016/0094-5765\(94\)00278-](https://doi.org/10.1016/0094-5765(94)00278-)  
18 T, 1995.

19 Crisp, D.: Measuring atmospheric carbon dioxide from space with the Orbiting Carbon Observatory-2 (OCO-2), *Proc. SPIE*,  
20 9607, 960702, doi: 10.1117/12.2187291, 2015.

21 de Foy, B., Lu, Z., Streets, D. G., Lamsal, L. N., and Duncan, B. N.: Estimates of power plant NO<sub>x</sub> emissions and lifetimes  
22 from OMI NO<sub>2</sub> satellite retrievals, *Atmos. Environ.*, 116, 1–11, 2015.

23 Duncan, B. N., Yoshida, Y., de Foy, B., Lamsal, L. N., Streets, D. G., Lu, Z., Pickering, K. E., and Krotkov, N. A.: The  
24 observed response of Ozone Monitoring Instrument (OMI) NO<sub>2</sub> columns to NO<sub>x</sub> emission controls on power plants in the  
25 United States: 2005–2011, *Atmos. Environ.*, 81, 102–111, 2013.

26 Fioletov, V. E., McLinden, C. A., Krotkov, N., Moran, M. D., and Yang, K.: Estimation of SO<sub>2</sub> emissions using OMI  
27 retrievals, *Geophys. Res. Lett.*, 38, L21811, doi: 10.1029/2011gl049402, 2011.

28 Gelaro, R., McCarty, W., Suárez, M. J., Todling, R., Molod, A., Takacs, L., Randles, C. A., Darmenov, A., Bosilovich, M.  
29 G., Reichle, R., Wargan, K., Coy, L., Cullather, R., Draper, C., Akella, S., Buchard, V., Conaty, A., Silva, A. M. d., Gu, W.,  
30 Kim, G.-K., Koster, R., Lucchesi, R., Merkova, D., Nielsen, J. E., Partyka, G., Pawson, S., Putman, W., Rienecker, M.,  
31 Schubert, S. D., Sienkiewicz, M., and Zhao, B.: The Modern-Era Retrospective Analysis for Research and Applications,  
32 Version 2 (MERRA-2), *J. Clim.*, 30, 5419–5454, doi: 10.1175/jcli-d-16-0758.1, 2017.

33 Glenn, C., Logan, T., Vu, B., Walsh, M., and Williams, P.: Evaluation of NO<sub>x</sub> Flue Gas Analyzers for Accuracy and Their  
34 Applicability for Low-Concentration Measurements AU - Gluck, Steven, J. *Air Waste Manage. Assoc.*, 53, 749–758, doi:  
35 10.1080/10473289.2003.10466208, 2003.

36 Goldberg, D. L., Saide, P. E., Lamsal, L. N., de Foy, B., Lu, Z., Woo, J. H., Kim, Y., Kim, J., Gao, M., Carmichael, G., and  
37 Streets, D. G.: A top-down assessment using OMI NO<sub>2</sub> suggests an underestimate in the NO<sub>x</sub> emissions inventory in Seoul,  
38 South Korea, during KORUS-AQ, *Atmos. Chem. Phys.*, 19, 1801–1818, doi: 10.5194/acp-19-1801-2019, 2019a.

39 [Goldberg, D. L., Lu, Z., Oda, T., Lamsal, L. N., Liu, F., Griffin, D., McLinden, C. A., Krotkov, N. A., Duncan, B. N., and](#)  
40 [Streets, D. G.: Exploiting OMI NO<sub>2</sub> satellite observations to infer fossil-fuel CO<sub>2</sub> emissions from U.S. megacities, \*Sci. Total\*  
41 \[Environ.\]\(#\), 695, 133805, doi: <https://doi.org/10.1016/j.scitotenv.2019.133805>, 2019b.](#)

1 [Goldberg, D. L., Lu, Z., Streets, D. G., de Foy, B., Griffin, D., McLinden, C. A., Lamsal, L. N., Krotkov, N. A., and Eskes,](#)  
2 [H.: Enhanced Capabilities of TROPOMI NO<sub>2</sub>: Estimating NO<sub>x</sub> from North American Cities and Power Plants, \*Environ. Sci.\*  
3 \[Technol.\]\(#\), doi: 10.1021/acs.est.9b04488, 2019c.](#)

4 Griffin, D., Zhao, X., McLinden, C. A., Boersma, F., Bourassa, A., Dammers, E., Degenstein, D., Eskes, H., Fehr, L.,  
5 Fioletov, V., Hayden, K., Kharol, S. K., Li, S.-M., Makar, P., Martin, R. V., Mihele, C., Mittermeier, R. L., Krotkov, N.,  
6 Sneep, M., Lamsal, L. N., Linden, M. t., Geffen, J. v., Veefkind, P., and Wolde, M.: High-resolution mapping of nitrogen  
7 dioxide with TROPOMI: First results and validation over the Canadian oil sands, *Geophys. Res. Lett.*, 46, 1049–1060, doi:  
8 10.1029/2018gl081095, 2019.

9 Hakkarainen, J., Ialongo, I., and Tamminen, J.: Direct space-based observations of anthropogenic CO<sub>2</sub> emission areas from  
10 OCO-2, *Geophys. Res. Lett.*, 43, 11,400–411,406, doi: 10.1002/2016GL070885, 2016.

11 [Hakkarainen, J., Ialongo, I., Maksyutov, S., and Crisp, D.: Analysis of Four Years of Global XCO<sub>2</sub> Anomalies as Seen by](#)  
12 [Orbiting Carbon Observatory-2, \*Remote Sensing\*, 11, 850, doi: 10.3390/rs11070850, 2019.](#)

13 Houweling, S., Baker, D., Basu, S., Boesch, H., Butz, A., Chevallier, F., Deng, F., Dlugokencky, E. J., Feng, L., Ganshin,  
14 A., Hasekamp, O., Jones, D., Maksyutov, S., Marshall, J., Oda, T., O'Dell, C. W., Oshchepkov, S., Palmer, P. I., Peylin, P.,  
15 Poussi, Z., Reum, F., Takagi, H., Yoshida, Y., and Zhuravlev, R.: An intercomparison of inverse models for estimating  
16 sources and sinks of CO<sub>2</sub> using GOSAT measurements, *Journal of Geophysical Research: Atmospheres*, 120, 5253–5266,  
17 doi:10.1002/2014JD022962, 2015.

18 [Ialongo, I., Virta, H., Eskes, H., Hovila, J., and Douros, J.: Comparison of TROPOMI/Sentinel 5 Precursor NO<sub>2</sub>](#)  
19 [observations with ground-based measurements in Helsinki, \*Atmos. Meas. Tech. Discuss.\*, \[https://doi.org/10.5194/amt-2019-\]\(https://doi.org/10.5194/amt-2019-329\)](#)  
20 [329, in review, 2019.](#)

21 Janardanan, R., Maksyutov, S., Oda, T., Saito, M., Kaiser, J. W., Ganshin, A., Stohl, A., Matsunaga, T., Yoshida, Y., and  
22 Yokota, T.: Comparing GOSAT observations of localized CO<sub>2</sub> enhancements by large emitters with inventory-based  
23 estimates, *Geophys. Res. Lett.*, 43, 3486–3493, doi: 10.1002/2016GL067843, 2016.

24 Janssens-Maenhout, G., Crippa, M., Guizzardi, D., Muntean, M., Schaaf, E., Dentener, F., Bergamaschi, P., Pagliari, V.,  
25 Olivier, J. G. J., Peters, J. A. H. W., van Aardenne, J. A., Monni, S., Doering, U., and Petrescu, A. M. R.: EDGAR v4.3.2  
26 global atlas of the three major greenhouse gas emissions for the period 1970–2012, *Earth Syst. Sci. Data Discuss.*, 2017, 1–  
27 55, doi: 10.5194/essd-2017-79, 2017.

28 [Jöckel, P., Tost, H., Pozzer, A., Kunze, M., Kirner, O., Brenninkmeijer, C. A. M., Brinkop, S., Cai, D. S., Dyroff, C.,](#)  
29 [Eckstein, J., Frank, F., Garny, H., Gottschaldt, K. D., Graf, P., Grewe, V., Kerkweg, A., Kern, B., Matthes, S., Mertens, M.,](#)  
30 [Meul, S., Neumaier, M., Nützel, M., Oberländer-Hayn, S., Ruhnke, R., Runde, T., Sander, R., Scharffe, D., and Zahn, A.:](#)  
31 [Earth System Chemistry integrated Modelling \(ESCiMo\) with the Modular Earth Submodel System \(MESSy\) version 2.51,](#)  
32 [Geosci. Model Dev.](#), 9, 1153–1200, doi: 10.5194/gmd-9-1153-2016, 2016.

33 Kleipool, Q. L., Dobber, M. R., de Haan, J. F., and Levelt, P. F.: Earth surface reflectance climatology from 3 years of OMI  
34 data, *Journal of Geophysical Research: Atmospheres*, 113, doi: 10.1029/2008jd010290, 2008.

35 Konovalov, I. B., Berezin, E. V., Ciais, P., Broquet, G., Zhuravlev, R. V., and Janssens-Maenhout, G.: Estimation of fossil-  
36 fuel CO<sub>2</sub> emissions using satellite measurements of “proxy” species, *Atmos. Chem. Phys.*, 16, 13509–13540,  
37 doi:10.5194/acp-16-13509-2016, 2016.

38 Kort, E. A., Frankenberg, C., Miller, C. E., and Oda, T.: Space-based observations of megacity carbon dioxide, *Geophys.*  
39 *Res. Lett.*, 39, L17806, doi: 10.1029/2012GL052738, 2012.

40 Krotkov, N. A., Lamsal, L. N., Celarier, E. A., Swartz, W. H., Marchenko, S. V., Bucsela, E. J., Chan, K. L., Wenig, M., and  
41 Zara, M.: The version 3 OMI NO<sub>2</sub> standard product, *Atmos. Meas. Tech.*, 10, 3133–3149, doi: 10.5194/amt-10-3133-2017,  
42 2017.



1 Levelt, P. F., van den Oord, G. H. J., Dobber, M. R., Malkki, A., Huib, V., Johan de, V., Stammes, P., Lundell, J. O. V., and  
2 Saari, H.: The ozone monitoring instrument, *Geoscience and Remote Sensing, IEEE Transactions on*, 44, 1093–1101, 2006.

3 Levelt, P. F., Joiner, J., Tamminen, J., Veefkind, J. P., Bhartia, P. K., Stein Zweers, D. C., Duncan, B. N., Streets, D. G.,  
4 Eskes, H., van der A, R., McLinden, C., Fioletov, V., Carn, S., de Laat, J., DeLand, M., Marchenko, S., McPeters, R.,  
5 Ziemke, J., Fu, D., Liu, X., Pickering, K., Apituley, A., González Abad, G., Arola, A., Boersma, F., Chan Miller, C., Chance,  
6 K., de Graaf, M., Hakkarainen, J., Hassinen, S., Ialongo, I., Kleipool, Q., Krotkov, N., Li, C., Lamsal, L., Newman, P.,  
7 Nowlan, C., Suleiman, R., Tilstra, L. G., Torres, O., Wang, H., and Wargan, K.: The Ozone Monitoring Instrument:  
8 overview of 14 years in space, *Atmos. Chem. Phys.*, 18, 5699–5745, doi: 10.5194/acp-18-5699-2018, 2018.

9 Liu, F., Zhang, Q., Tong, D., Zheng, B., Li, M., Huo, H., and He, K. B.: High-resolution inventory of technologies,  
10 activities, and emissions of coal-fired power plants in China from 1990 to 2010, *Atmos. Chem. Phys.*, 15, 13299–13317, doi:  
11 10.5194/acp-15-13299-2015, 2015.

12 Liu, F., Beirle, S., Zhang, Q., Dörner, S., He, K., and Wagner, T.: NO<sub>x</sub> lifetimes and emissions of cities and power plants in  
13 polluted background estimated by satellite observations, *Atmos. Chem. Phys.*, 16, 5283–5298, doi: 10.5194/acp-16-5283-  
14 2016, 2016.

15 Liu, F., Beirle, S., Zhang, Q., van der A, R. J., Zheng, B., Tong, D., and He, K.: NO<sub>x</sub> emission trends over Chinese cities  
16 estimated from OMI observations during 2005 to 2015, *Atmos. Chem. Phys.*, 17, 9261–9275, doi: 10.5194/acp-17-9261-  
17 2017, 2017.

18 [Liu, F., Choi, S., Li, C., Fioletov, V. E., McLinden, C. A., Joiner, J., Krotkov, N. A., Bian, H., Janssens-Maenhout, G.,  
19 Darmenov, A. S., and da Silva, A. M.: A new global anthropogenic SO<sub>2</sub> emission inventory for the last decade: a mosaic of  
20 satellite-derived and bottom-up emissions, \*Atmos. Chem. Phys.\*, 18, 16571–16586, doi: 10.5194/acp-18-16571-2018, 2018.](#)

21 Lu, Z., and Streets, D. G.: Increase in NO<sub>x</sub> emissions from Indian thermal power plants during 1996–2010: Unit-based  
22 inventories and multisatellite observations, *Environ. Sci. Technol.*, 46, 7463–7470, doi: 10.1021/es300831w, 2012.

23 Lu, Z., Streets, D. G., de Foy, B., and Krotkov, N. A.: Ozone Monitoring Instrument observations of interannual increases in  
24 SO<sub>2</sub> emissions from Indian coal-fired power plants during 2005–2012, *Environ. Sci. Technol.*, 47, 13993–14000, 2013.

25 Lu, Z., Streets, D. G., de Foy, B., Lamsal, L. N., Duncan, B. N., and Xing, J.: Emissions of nitrogen oxides from US urban  
26 areas: estimation from Ozone Monitoring Instrument retrievals for 2005–2014, *Atmos. Chem. Phys.*, 15, 10367–10383, doi:  
27 10.5194/acp-15-10367-2015, 2015.

28 Majanne, Y., Korpela, T., Judl, J., Koskela, S., Laukkanen, V., and Häyrinen, A.: Real Time Monitoring of Environmental  
29 Efficiency of Power Plants, *IFAC-PapersOnLine*, 48, 495–500, doi: <https://doi.org/10.1016/j.ifacol.2015.12.428>, 2015.

30 Makgato, S., and Chirwa, E.: Characteristics of Thermal Coal used by Power Plants in Waterberg Region of South Africa,  
31 *Chemical Engineering Transactions*, 57, 511–516, 10.3303/CET1757086, 2017.

32 McLinden, C. A., Fioletov, V., Boersma, K. F., Kharol, S. K., Krotkov, N., Lamsal, L., Makar, P. A., Martin, R. V.,  
33 Veefkind, J. P., and Yang, K.: Improved satellite retrievals of NO<sub>2</sub> and SO<sub>2</sub> over the Canadian oil sands and comparisons  
34 with surface measurements, *Atmos. Chem. Phys.*, 14, 3637–3656, doi: 10.5194/acp-14-3637-2014, 2014.

35 Nassar, R., Hill, T. G., McLinden, C. A., Wunch, D., Jones, D. B. A., and Crisp, D.: Quantifying CO<sub>2</sub> Emissions From  
36 Individual Power Plants From Space, *Geophys. Res. Lett.*, 44, 10,045–010,053, doi:10.1002/2017GL074702, 2017.

37 [Oda, T., Maksyutov, S., and Andres, R. J.: The Open-source Data Inventory for Anthropogenic CO<sub>2</sub>, version 2016  
38 \(ODIAC2016\): a global monthly fossil fuel CO<sub>2</sub> gridded emissions data product for tracer transport simulations and surface  
39 flux inversions, \*Earth Syst. Sci. Data\*, 10, 87–107, doi: 10.5194/essd-10-87-2018, 2018.](#)

40 Pretorius, I., Piketh, S., Burger, R., and Neomagus, H.: A perspective on South African coal fired power station emissions,  
41 *Journal of Energy in Southern Africa*, 26, 27–40, doi: 10.17159/2413-3051/2015/v26i3a2127, 2015.

1 Reuter, M., Buchwitz, M., Hilboll, A., Richter, A., Schneising, O., Hilker, M., Heymann, J., Bovensmann, H., and Burrows,  
2 J. P.: Decreasing emissions of NO<sub>x</sub> relative to CO<sub>2</sub> in East Asia inferred from satellite observations, *Nature Geoscience*, 7,  
3 792, doi: 10.1038/ngeo2257, 2014.

4 Reuter, M., Buchwitz, M., Schneising, O., Krautwurst, S., O'Dell, C. W., Richter, A., Bovensmann, H., and Burrows, J. P.:  
5 Towards monitoring localized CO<sub>2</sub> emissions from space: co-located regional CO<sub>2</sub> and NO<sub>2</sub> enhancements observed by the  
6 OCO-2 and S5P satellites, *Atmos. Chem. Phys. Discuss.*, 19, 9371–9383, doi: 10.5194/acp-19-9371-2019-15, in review,  
7 2019.

8 Russell, A. R., Perring, A. E., Valin, L. C., Bucsela, E. J., Browne, E. C., Wooldridge, P. J., and Cohen, R. C.: A high spatial  
9 resolution retrieval of NO<sub>2</sub> column densities from OMI: method and evaluation, *Atmos. Chem. Phys.*, 11, 8543–8554, doi:  
10 10.5194/acp-11-8543-2011, 2011.

11 Schneising, O., Heymann, J., Buchwitz, M., Reuter, M., Bovensmann, H., and Burrows, J. P.: Anthropogenic carbon dioxide  
12 source areas observed from space: assessment of regional enhancements and trends, *Atmos. Chem. Phys.*, 13, 2445–2454,  
13 doi: 10.5194/acp-13-2445-2013, 2013.

14 Schoeberl, M. R., Douglass, A. R., Hilsenrath, E., Bhartia, P. K., Beer, R., Waters, J. W., Gunson, M. R., Froidevaux, L.,  
15 Gille, J. C., and Barnett, J. J.: Overview of the EOS Aura mission, *Geoscience and Remote Sensing, IEEE Transactions on*,  
16 44, 1066–1074, 2006.

17 Shaiganfar, R., Beirle, S., Denier van der Gon, H., Jonkers, S., Kuenen, J., Petetin, H., Zhang, Q., Beekmann, M., and  
18 Wagner, T.: Estimation of the Paris NO<sub>x</sub> emissions from mobile MAX-DOAS observations and CHIMERE model  
19 simulations during the MEGAPOLI campaign using the closed integral method, *Atmos. Chem. Phys.*, 17, 7853–7890, doi:  
20 10.5194/acp-17-7853-2017, 2017.

21 Shindell, D., and Faluvegi, G.: The net climate impact of coal-fired power plant emissions, *Atmos. Chem. Phys.*, 10, 3247–  
22 3260, doi: 10.5194/acp-10-3247-2010, 2010.

23 Sloss, L.: Efficiency and emissions monitoring and reporting, CCC/188, 40, IEA Clean Coal Centre, London, UK, 2011.

24 Tong, D., Zhang, Q., Davis, S. J., Liu, F., Zheng, B., Geng, G., Xue, T., Li, M., Hong, C., Lu, Z., Streets, D. G., Guan, D.,  
25 and He, K.: Targeted emission reductions from global super-polluting power plant units, *Nature Sustainability*, 1, 59–68, doi:  
26 10.1038/s41893-017-0003-y, 2018.

27 U.S. Energy Information Administration (USEIA), *Electric Power Annual 2017*, available at  
28 <https://www.eia.gov/electricity/annual/pdf/epa.pdf> (last access: April 11, 2019), 2018.

29 U.S. Environmental Protection Agency (USEPA), *Compilation of Air Pollutant Emission Factors, AP-42, Fifth Edition*,  
30 Volume 1, Chapter 1, Washington, D. C., available at: <https://www3.epa.gov/ttn/chief/ap42/ch01/index.html> (last access:  
31 March 20, 2019), 2009.

32 U.S. Environmental Protection Agency (USEPA): *Technical support document for eGRID with year 2016 data (the*  
33 *Emissions & Generation Resource Integrated Database)*, Washington, D.C., 2018.

34 Valin, L. C., Russell, A. R., and Cohen, R. C.: Variations of OH radical in an urban plume inferred from NO<sub>2</sub> column  
35 measurements, *Geophys. Res. Lett.*, 40, 1856–1860, doi:10.1002/grl.50267, 2013.

36 Varon, D. J., Jacob, D. J., McKeever, J., Jervis, D., Durak, B. O. A., Xia, Y., and Huang, Y.: Quantifying methane point  
37 sources from fine-scale satellite observations of atmospheric methane plumes, *Atmos. Meas. Tech.*, 11, 5673–5686, doi:  
38 10.5194/amt-11-5673-2018, 2018.

39 Veefkind, J. P., Aben, I., McMullan, K., Förster, H., de Vries, J., Otter, G., Claas, J., Eskes, H. J., de Haan, J. F., Kleipool,  
40 Q., van Weele, M., Hasekamp, O., Hoogeveen, R., Landgraf, J., Snel, R., Tol, P., Ingmann, P., Voors, R., Kruizinga, B.,  
41 Vink, R., Visser, H., and Levelt, P. F.: TROPOMI on the ESA Sentinel-5 Precursor: A GMES mission for global  
42 observations of the atmospheric composition for climate, air quality and ozone layer applications, *Remote Sens. Environ.*,  
43 120, 70–83, 2012.

- 1 Velazco, V. A., Buchwitz, M., Bovensmann, H., Reuter, M., Schneising, O., Heymann, J., Krings, T., Gerilowski, K., and  
2 Burrows, J. P.: Towards space based verification of CO<sub>2</sub> emissions from strong localized sources: fossil fuel power plant  
3 emissions as seen by a CarbonSat constellation, *Atmos. Meas. Tech.*, 4, 2809–2822, doi: 10.5194/amt-4-2809-2011, 2011.
- 4 [Wang, S., Zhang, Y., Hakkarainen, J., Ju, W., Liu, Y., Jiang, F., and He, W.: Distinguishing anthropogenic CO<sub>2</sub> emissions](#)  
5 [From different energy intensive industrial sources using OCO-2 observations: A case study in Northern China, \*Journal of\*](#)  
6 [Geophysical Research: Atmospheres](#), 123, 9462–9473, doi: 10.1029/2018jd029005, 2018.
- 7 Wheeler, D., and Ummel, K.: Calculating CARMA: Global estimation of CO<sub>2</sub> emissions from the power sector, Center for  
8 Global Development, Working Paper 145, 2008.
- 9 Yokota, T., Yoshida, Y., Eguchi, N., Ota, Y., Tanaka, T., Watanabe, H., and Maksyutov, S.: Global Concentrations of CO<sub>2</sub>  
10 and CH<sub>4</sub> Retrieved from GOSAT: First Preliminary Results, *SOLA*, 5, 160–163, doi: 10.2151/sola.2009-041, 2009.

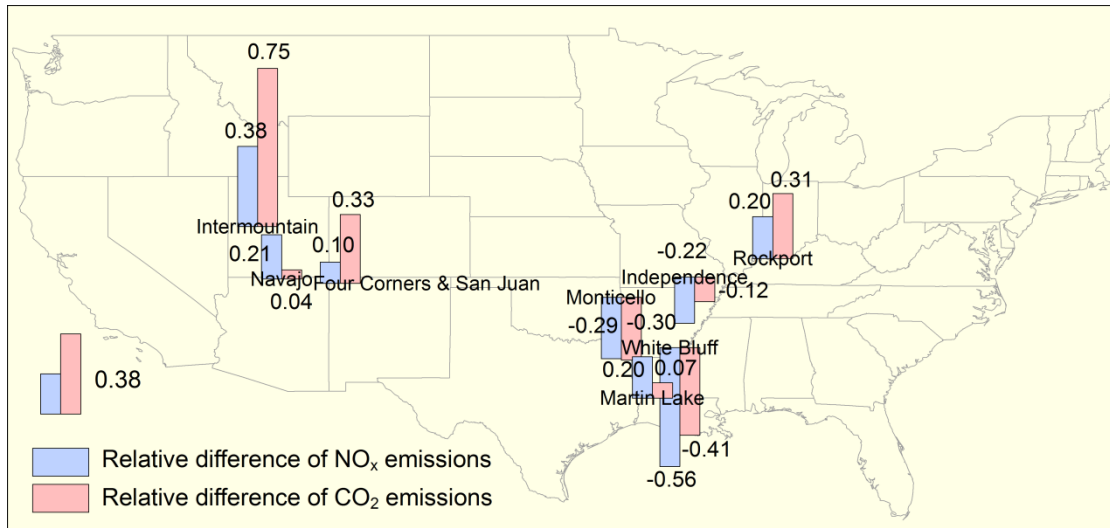
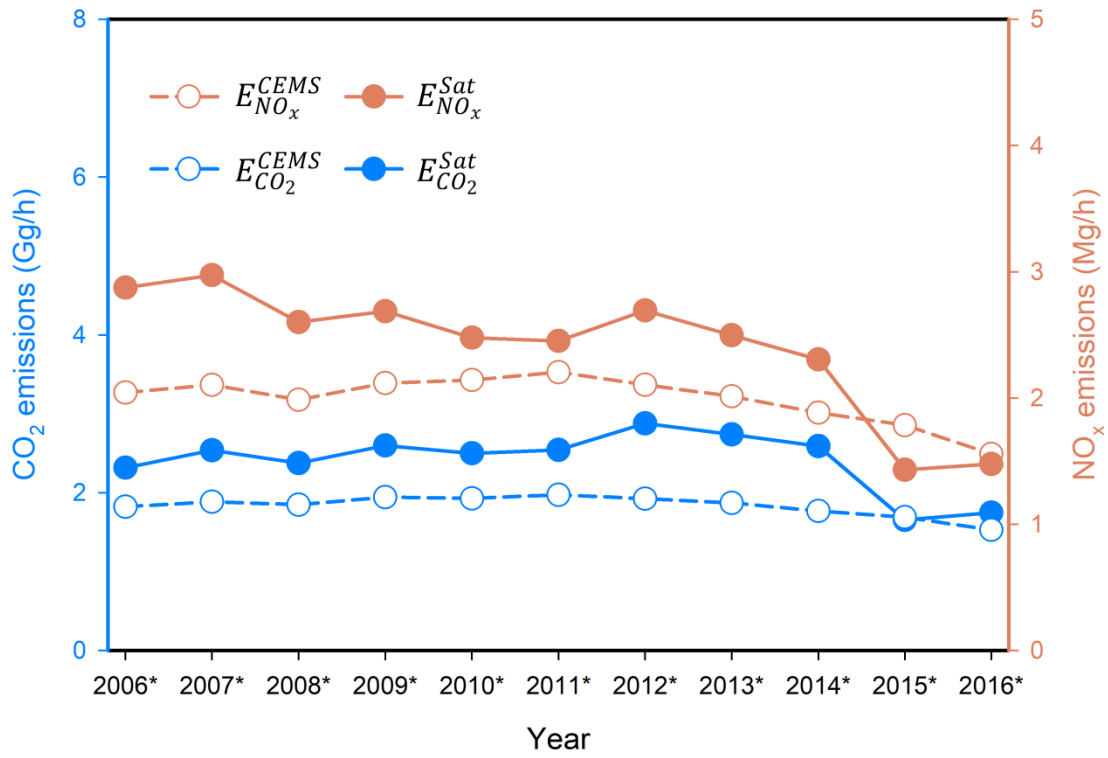
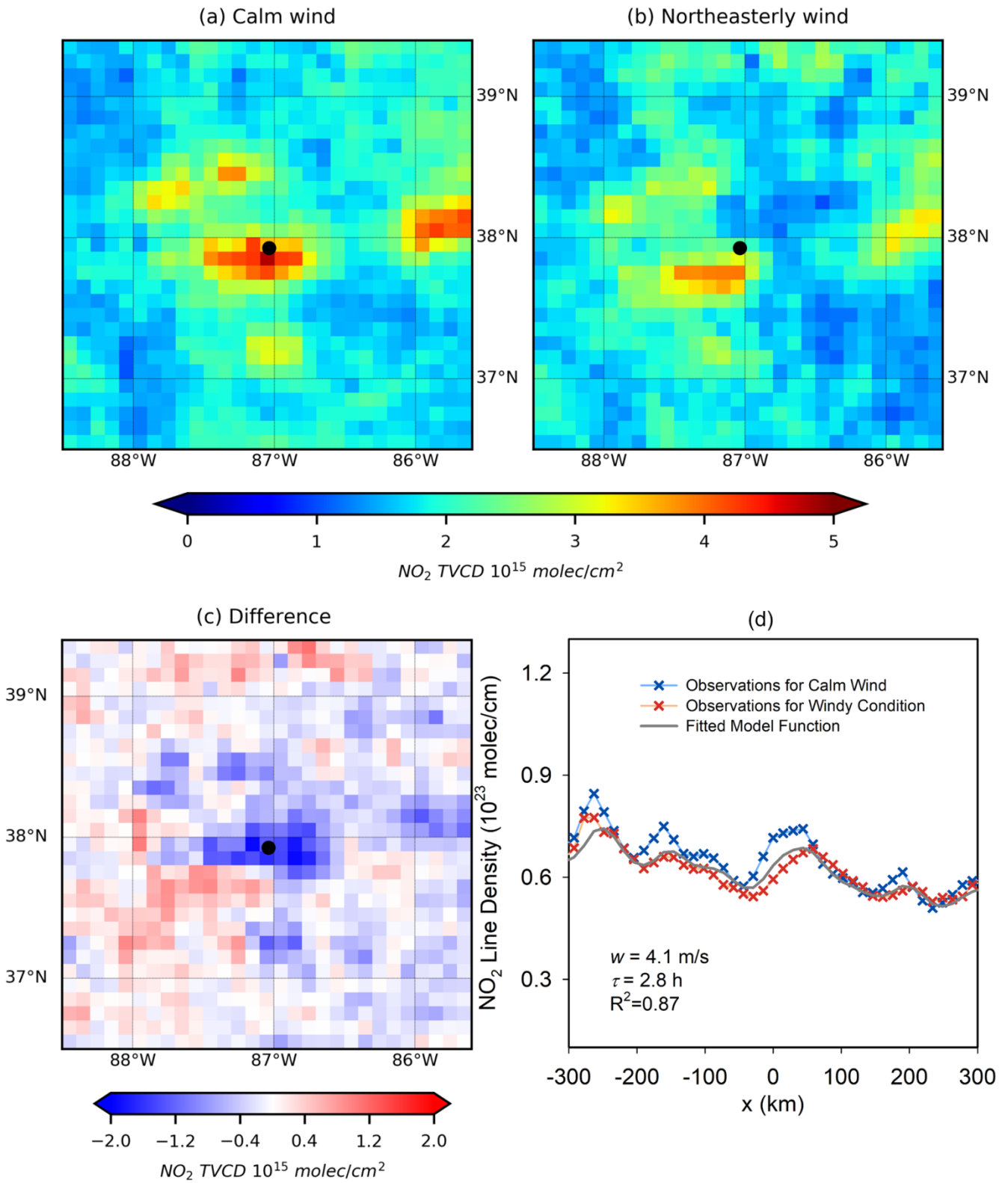
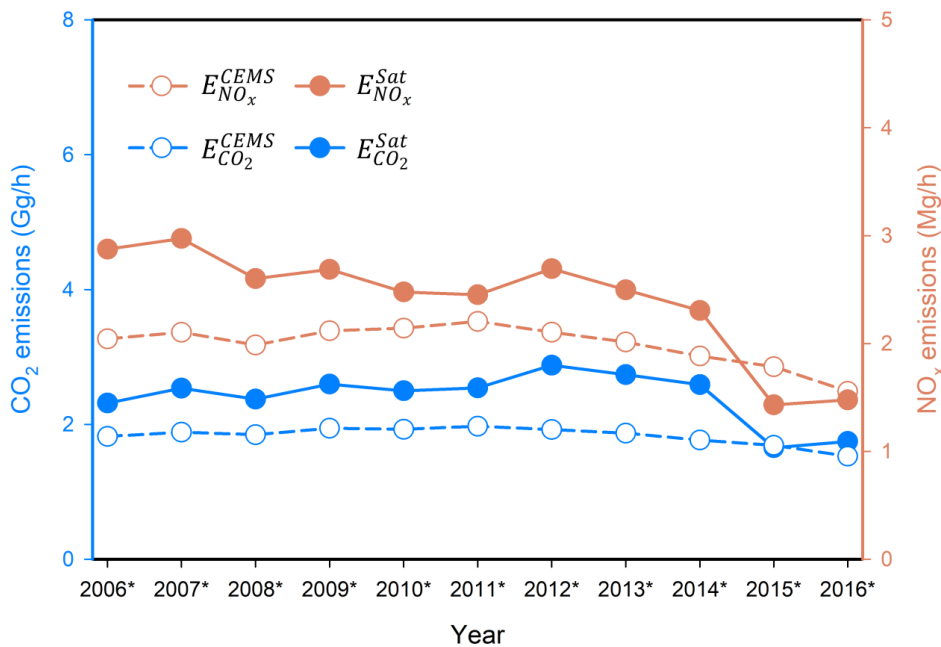


**Figure 1** Locations of the power plants investigated in this study. The bar charts denote the relative differences, defined as  $(E^{Sat} - E^{CEMS})/E^{CEMS}$ , averaged over 2005–2017, for NO<sub>x</sub> (blue) and CO<sub>2</sub> (red) emissions. The upward and downward bars represent positive and negative differences, respectively. The Monticello power plant installed SNCR to control NO<sub>x</sub> emissions in 2008. The other power plants are not equipped with post-combustion NO<sub>x</sub> control devices.

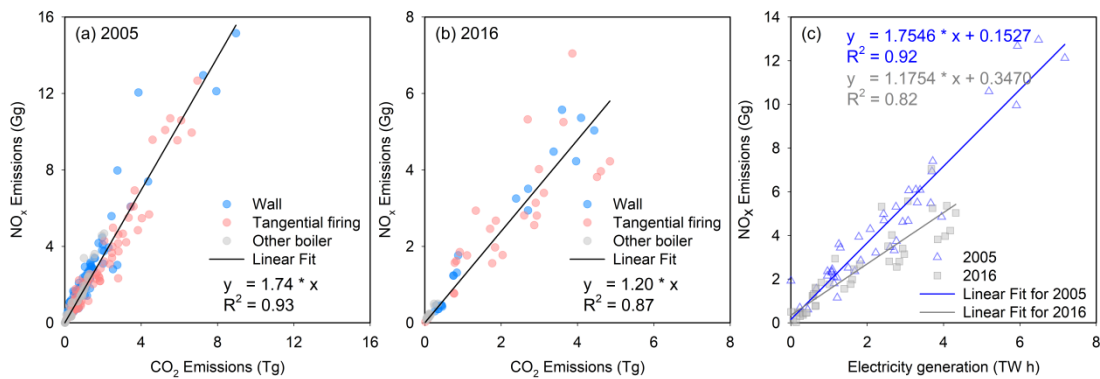


1  
2 **Figure 2** Mean OMI  $\text{NO}_2$  tropospheric VCDs around the Rockport power plant (Indiana, USA) for (a) calm conditions, (b) northeasterly  
3 wind and (c) their difference (northeasterly – calm) for the period of 2005 – 2017. The location of Rockport is labelled by a black dot. (d)  
4  $\text{NO}_2$  line densities around Rockport. Crosses:  $\text{NO}_2$  line densities for calm (blue) and northeasterly winds (red) as function of the distance  $x$   
5 to Rockport center. Grey line: the fitted results for  $\text{NO}_2$  line densities for northeasterly winds. The numbers indicate the net mean wind  
6 velocities (windy – calm) from MERRA-2 ( $w$ ), the fitted lifetime ( $\tau$ ), and the coefficient of determination ( $R^2$ ) of the fit.

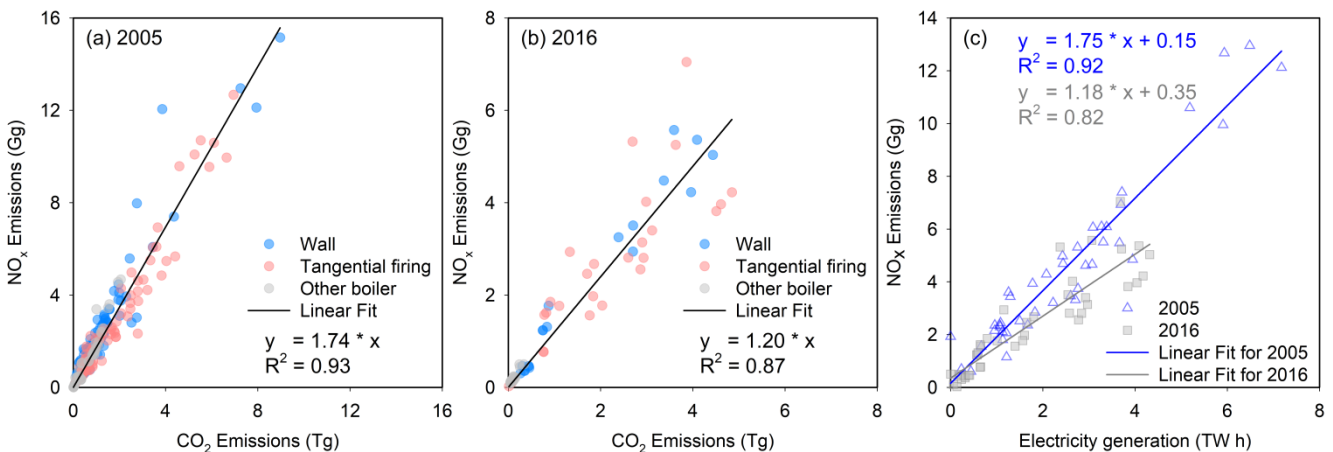


1  
 2 **Figure 3**  $E_{NO_x}^{Sat}$  (Mg/h; orange solid lines – right axis) and  $E_{CO_2}^{Sat}$  (Gg/h; blue solid line – left axis) for the Rockport power plant during  
 3 from 2005 to 2017.  $E_{NO_x}^{CEMS}$  and  $E_{CO_2}^{CEMS}$  (dashed lines) are also shown. The 3-year periods are represented by the middle year with an  
 4 asterisk (e.g., 2006\* denotes the period from 2005 to 2007).

5



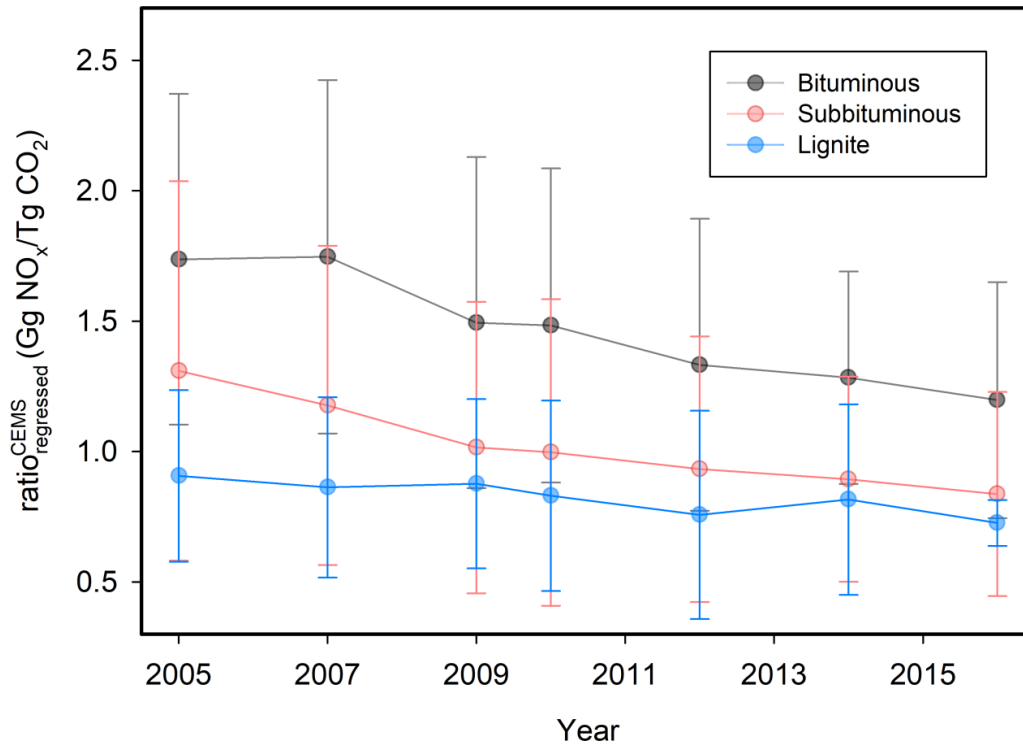
6



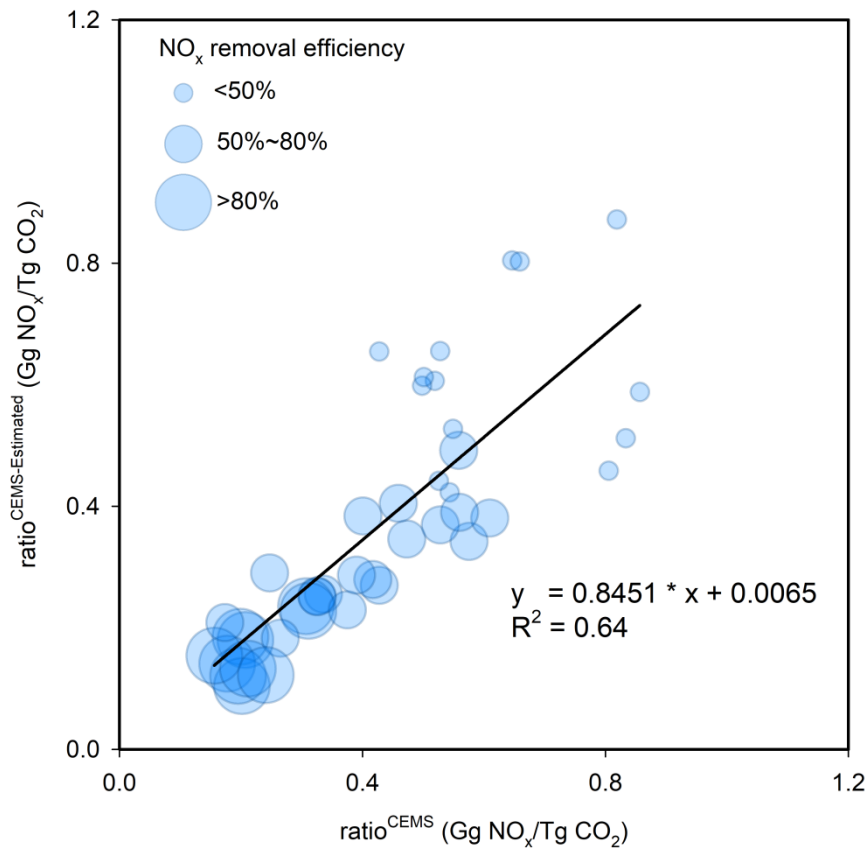
7

8 **Figure 24** Scatter plots of  $E_{NO_x}^{CEMS}$  versus  $E_{CO_2}^{CEMS}$  for all the US bituminous coal-fired electric generating units for (a) 2005 and (b) 2016.  
 9 Values are color coded by firing type. (c) Scatter plot of  $E_{NO_x}^{CEMS}$  versus electricity generation of the same units for years 2005 (triangle) and  
 10 2016 (square). Only plants without post-combustion  $NO_x$  control devices within a given year are used. The electricity generation data are  
 11 also from eGRID. The lines in all three panels represent the computed linear regressions.

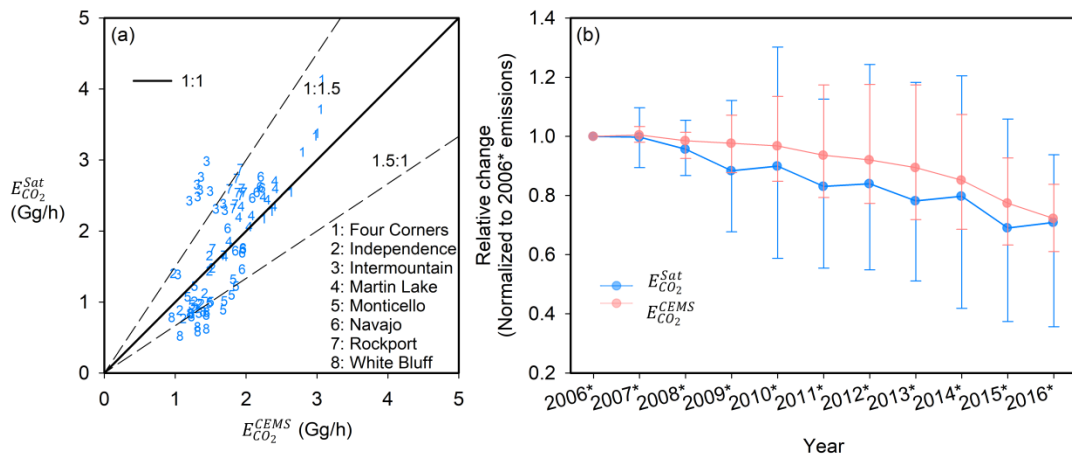
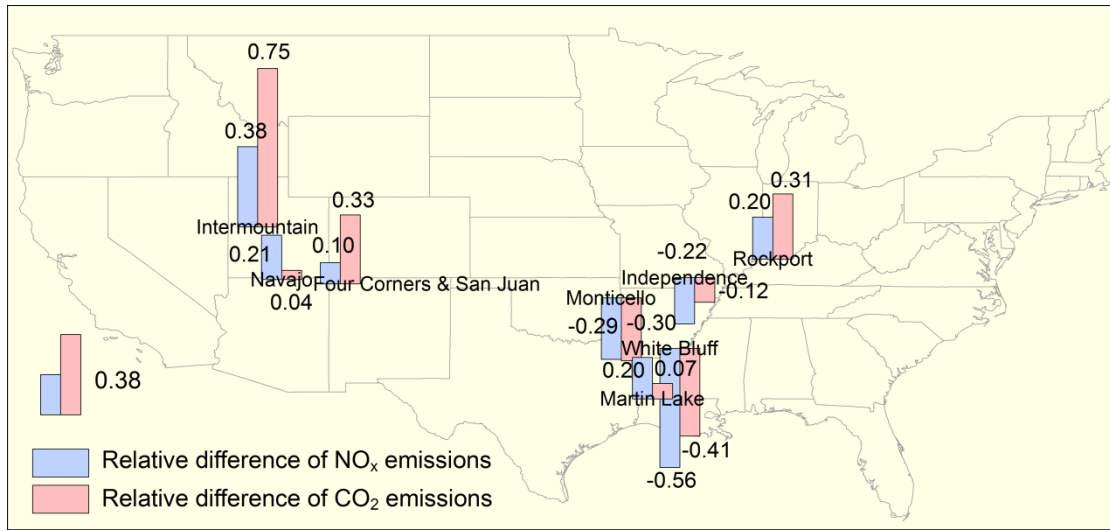
12



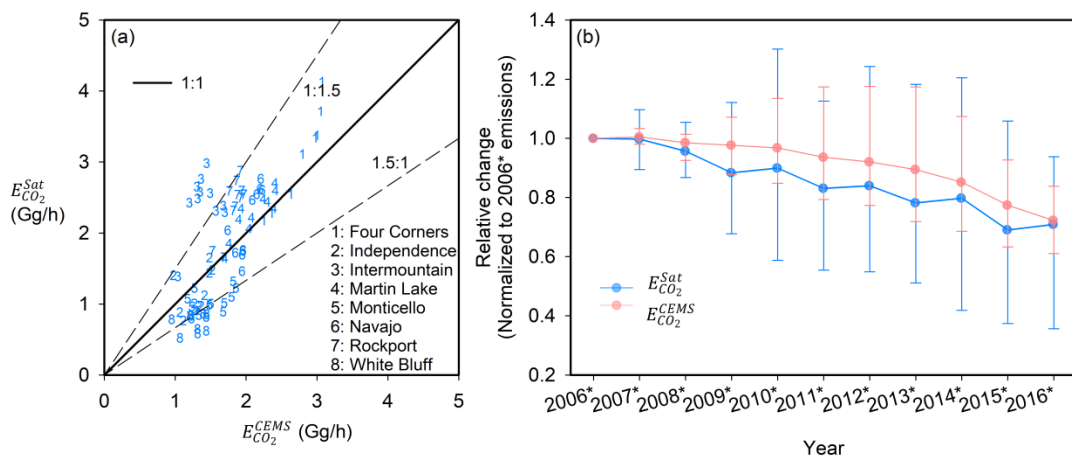
1  
 2 | **Figure 35** Interannual trends of  $ratio_{regressed}^{CEMS}$  for power plants using bituminous, subbituminous and lignite coal types and without post-  
 3 combustion  $NO_x$  control devices in a given year. Error bars show the standard deviations for ratios of  $E_{NO_x}^{CEMS}$  to  $E_{CO_2}^{CEMS}$  for individual power  
 4 plants.



5  
 6 | **Figure 46** Scatterplot of ~~the ratio of~~  $ratio^{CEMS-Estimated}$  as compared to  $ratio^{CEMS}$  for 2016. All 44 coal-fired power plants that  
 7 operated post-combustion ~~techniques/devices~~ after 2005 and before 2016 (including 2016) are used in the plot. The sizes of the circles  
 8 denote the magnitude of the  $NO_x$  reduction efficiency of post-combustion control devices estimated in this study. The line represents the  
 9 linear regression of  $ratio^{CEMS}$  to  $ratio^{CEMS-Estimated}$ .

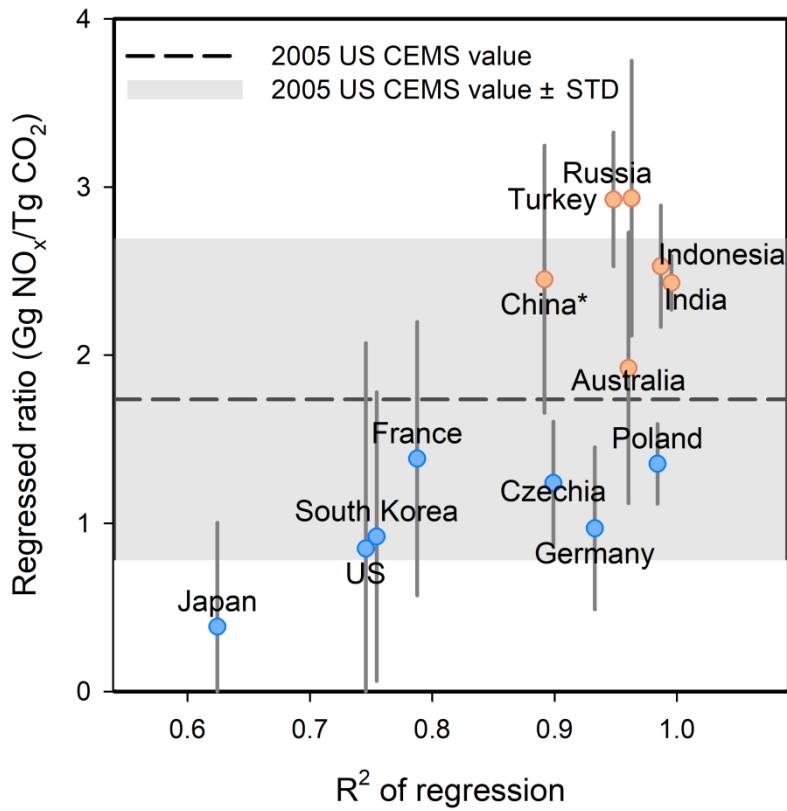


**Figure 5** The bar charts denote the relative differences, defined as  $(E_{CO_2}^{Sat} - E_{CO_2}^{CEMS}) / E_{CO_2}^{CEMS}$ , averaged over 2005–2017, for  $NO_x$  (blue) and  $CO_2$  (red) emissions. The upward and downward bars represent positive and negative differences, respectively. The Monticello power plant installed SNCR to control  $NO_x$  emissions in 2008. Other power plants are not equipped with post-combustion  $NO_x$  control devices.

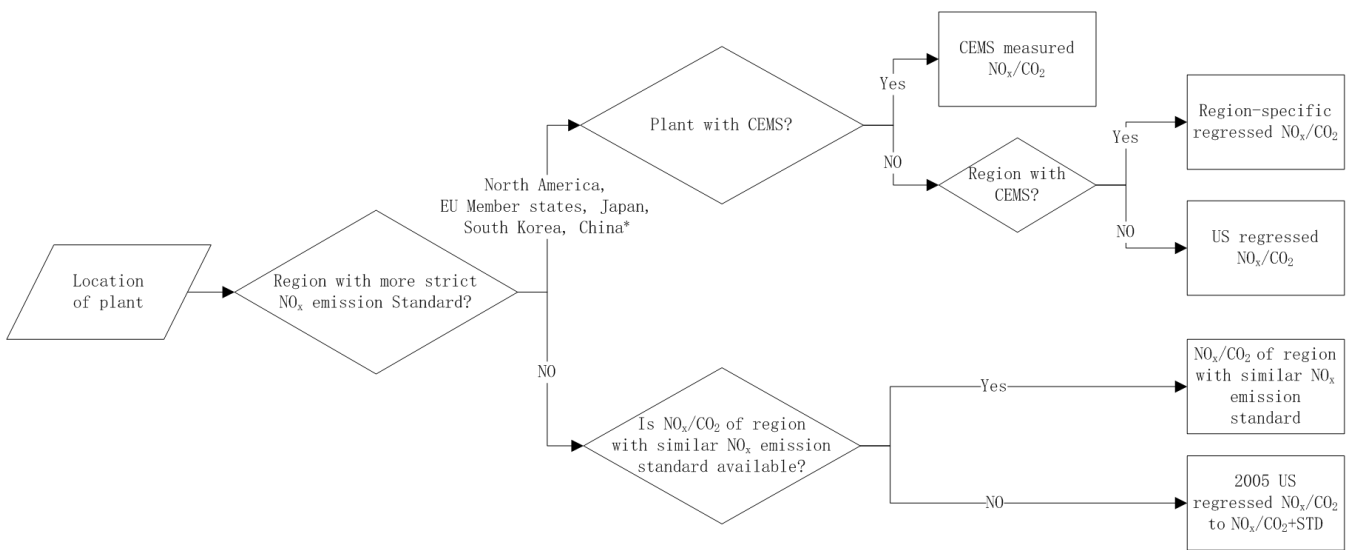


**Figure 67** (a) Scatterplot of  $E_{CO_2}^{Sat}$  for eight power plants as compared to  $E_{CO_2}^{CEMS}$  from 2006\* to 2016\*. The straight solid and lines represent the ratio of 1:1. The dashed lines represent the ratio of 1:1.5 and 1.5:1, respectively. (b) Interannual trends of the averaged  $E_{CO_2}^{Sat}$  (blue lines) and  $E_{CO_2}^{CEMS}$  (pink lines) are for all power plants analyzed in this study from 2006\*–2016\*, as normalized to the 2006\* value. The whiskers denote the maximum and minimum values.



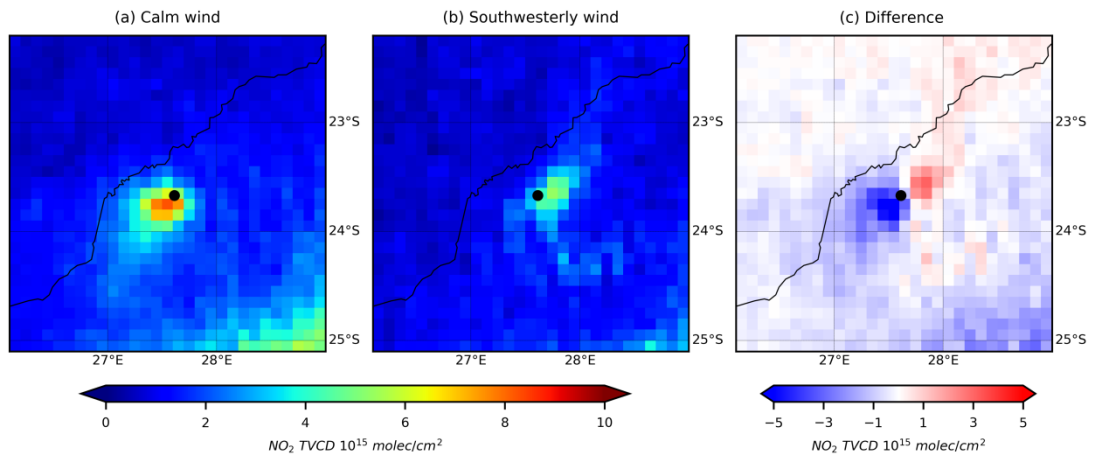


**Figure 8** Comparison of the regressed NO<sub>x</sub> to CO<sub>2</sub> emission ratios derived from the global power emissions database (GPED) for different regions versus the correlation coefficient of the regression. The blue and red circles denote regions that are subject to more strict standard for NO<sub>x</sub> emissions from power plants (i.e., a NO<sub>x</sub> ELV of 200 mg/m<sup>3</sup> or less) and other regions, respectively. Y axis: the slope of the regression of the NO<sub>x</sub> to CO<sub>2</sub> emissions with an assumed y-intercept of zero. Error bars show the standard deviations for the NO<sub>x</sub> to CO<sub>2</sub> emission ratios for individual power plants. X axis: correlation coefficient of the regression. The dashed line represents 2005 US  $ratio_{regressed}^{CEMS}$  for bituminous coal derived in this study. The grey shadow represents 2005 US  $ratio_{regressed}^{CEMS} \pm$  standard deviation. \*China switched from being a less strict country to a more strict country in 2014, when most coal-fired power plants in China were required to comply with its new emission standards (GB13223-2011).

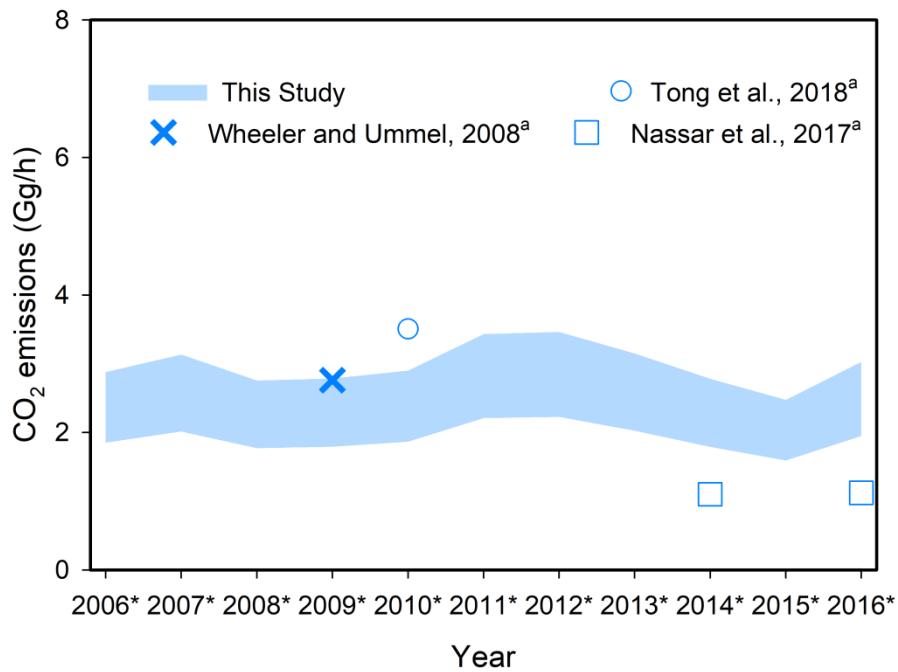


**Figure 9** Schematic of our methodology to estimate the NO<sub>x</sub> to CO<sub>2</sub> emission ratios for power plants outside the US.

\*China switched from being a less strict country to a more strict country in 2014, when most coal-fired power plants in China were required to comply with its new emission standards (GB13223-2011).



**Figure 10** Mean OMI NO<sub>2</sub> tropospheric VCDs around the Matimba power plant (Lephalale, South Africa) for (a) calm, (b) southwesterly wind conditions and (c) their difference (southwesterly – calm) for the period of 2005 – 2017. The location of Matimba is **labelled** represented by a black dot.



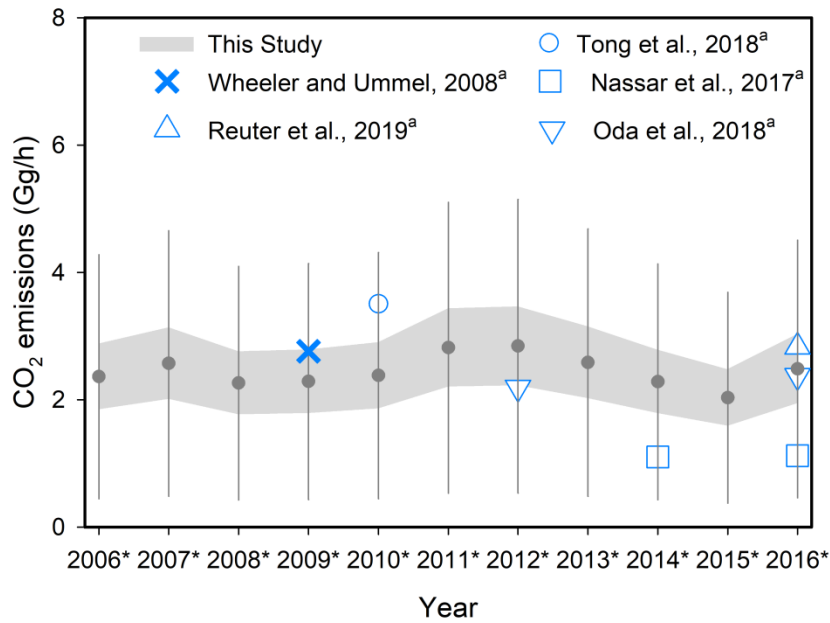


**Figure 811** Comparison of  $E_{CO_2}^{Sat}$  (Gg/h) derived in this study with existing estimates for the Matimba power plant during 2005 to 2017.  $E_{CO_2}^{Sat}$  is inferred based on the  $NO_x$  to  $CO_2$  emissions ratio ranging from  $ratio_{regressed}^{CEMS}$  to  $ratio_{regressed}^{CEMS} + \text{standard deviation of ratio}$ . The upper and lower grey bands denote the emissions inferred from  $ratio_{regressed}^{CEMS}$  and  $ratio_{regressed}^{CEMS} + \text{standard deviation of ratio}$ , respectively. The grey dots and error bars show the mean of the upper and lower grey bands and their uncertainties, respectively.  
<sup>a</sup>Emissions are estimated for 2009 by Wheeler and Ummel (2008); for 2010 by Tong et al. (2018); and for 2014 and 2016 by Nassar et al. (2017); for 2016 by Reuter et al. (2019); and for 2012 and 2016 by Oda et al. (2018).

**Table 1** The slope ( $ratio_{regressed}^{CEMS}$ ), coefficient of determination, standard deviation and sample number of the linear regression of  $E_{NO_x}^{CEMS}$  and  $E_{CO_2}^{CEMS}$  by year for all US power plants without post-combustion NO<sub>x</sub> control devices from 2005 to 2016.

| Coal type     | Year | $ratio_{regressed}^{CEMS}$ | R <sup>2</sup> | Standard deviation | Sample number <sup>a</sup> |
|---------------|------|----------------------------|----------------|--------------------|----------------------------|
| Bituminous    | 2005 | 1.74                       | 0.93           | 0.63               | 278                        |
|               | 2007 | 1.75                       | 0.91           | 0.68               | 286                        |
|               | 2009 | 1.49                       | 0.88           | 0.64               | 241                        |
|               | 2010 | 1.48                       | 0.86           | 0.60               | 235                        |
|               | 2012 | 1.33                       | 0.87           | 0.56               | 190                        |
|               | 2014 | 1.28                       | 0.87           | 0.41               | 136                        |
|               | 2016 | 1.20                       | 0.87           | 0.45               | 66                         |
| Subbituminous | 2005 | 1.31                       | 0.65           | 0.73               | 226                        |
|               | 2007 | 1.18                       | 0.61           | 0.61               | 221                        |
|               | 2009 | 1.02                       | 0.66           | 0.56               | 230                        |
|               | 2010 | 1.00                       | 0.67           | 0.59               | 216                        |
|               | 2012 | 0.93                       | 0.74           | 0.51               | 200                        |
|               | 2014 | 0.89                       | 0.74           | 0.39               | 165                        |
|               | 2016 | 0.84                       | 0.70           | 0.39               | 111                        |
| Lignite       | 2005 | 0.91                       | 0.74           | 0.33               | 20                         |
|               | 2007 | 0.86                       | 0.82           | 0.35               | 22                         |
|               | 2009 | 0.88                       | 0.91           | 0.32               | 16                         |
|               | 2010 | 0.83                       | 0.94           | 0.37               | 18                         |
|               | 2012 | 0.76                       | 0.91           | 0.40               | 15                         |
|               | 2014 | 0.82                       | 0.92           | 0.37               | 12                         |
|               | 2016 | 0.73                       | 0.78           | 0.09               | 9                          |

<sup>a</sup>The sample number generally decreases from 2005 to 2016 as power plants installed post-combustion NO<sub>x</sub> control devices over time.

**Table 2** Summary of effective NO<sub>x</sub> lifetimes, satellite-derived NO<sub>x</sub> emissions ( $E_{NO_x}^{Sat}$ ), CO<sub>2</sub> emissions ( $E_{CO_2}^{Sat}$ ) and bottom-up NO<sub>x</sub> emissions ( $E_{NO_x}^{CEMS}$ ), CO<sub>2</sub> emissions ( $E_{CO_2}^{CEMS}$ ) for 8 US power plants during May to September from 2005 to 2017. The 3-year periods are represented by the middle year with an asterisk.

| Category   | Year                        | Four Corners<br>& San Juan | Independence | Intermountain | Martin Lake | Monticello | Navajo | Rockport | White Bluff |     |
|--|-----------------------------|----------------------------|--------------|---------------|-------------|------------|--------|----------|-------------|-----|
| NO <sub>x</sub> lifetime                               | 2005-2017                   | 2.7                        | 2.5          | 2.2           | 2.3         | 3.2        | 2.3    | 2.4      | 4.3         |     |
| $E_{NO_x}^{Sat}$<br>(Mg/h)                             | 2006*                       | 10.5                       | 2.0          | 4.0           | 2.4         | 1.1        | 4.6    | 2.9      | 1.0         |     |
|  | 2007*                       | 10.0                       | 1.7          | 4.1           | 2.3         | 1.1        | 4.4    | 3.0      | 0.9         |     |
|  | 2008*                       | 9.4                        | 1.6          | 3.7           | 2.0         | 0.8        | 4.5    | 2.6      | 0.9         |     |
|  | 2009*                       | 7.2                        | 1.2          | 3.9           | 2.1         | 0.7        | 3.9    | 2.7      | 0.7         |     |
|  | 2010*                       | 6.8                        | 1.0          | 4.4           | 2.1         | 0.6        | 3.6    | 2.5      | 0.9         |     |
|  | 2011*                       | 6.5                        | 0.9          | 3.6           | 1.8         | 0.7        | 2.5    | 2.5      | 0.8         |     |
|  | 2012*                       | 6.3                        | 0.9          | 3.4           | 1.6         | 0.6        | 2.3    | 2.7      | 0.8         |     |
|  | 2013*                       | 5.6                        | 0.8          | 3.5           | 1.8         | 0.5        | 1.9    | 2.5      | 0.6         |     |
|  | 2014*                       | 4.4                        | 0.7          | 3.5           | 1.7         | 0.8        | 2.2    | 2.3      | 0.5         |     |
|  | 2015*                       | 3.8                        | 0.8          | 3.0           | 1.4         | 0.7        | 2.1    | 1.4      | 0.4         |     |
| $E_{NO_x}^{CEMS}$<br>(Mg/h)                            | 2006*                       | 7.4                        | 1.8          | 3.0           | 1.8         | 1.5        | 3.8    | 2.0      | 1.7         |     |
|  | 2007*                       | 7.3                        | 1.8          | 3.1           | 1.8         | 1.4        | 3.9    | 2.1      | 1.6         |     |
|  | 2008*                       | 6.8                        | 1.8          | 2.9           | 1.8         | 1.3        | 3.8    | 2.0      | 1.6         |     |
|  | 2009*                       | 6.5                        | 1.6          | 2.9           | 1.8         | 1.2        | 3.4    | 2.1      | 1.8         |     |
|  | 2010*                       | 6.2                        | 1.6          | 2.8           | 1.7         | 1.1        | 2.8    | 2.1      | 1.8         |     |
|  | 2011*                       | 6.2                        | 1.4          | 2.5           | 1.5         | 1.0        | 2.2    | 2.2      | 1.9         |     |
|  | 2012*                       | 6.1                        | 1.3          | 2.4           | 1.4         | 0.9        | 1.9    | 2.1      | 1.9         |     |
|  | 2013*                       | 5.6                        | 1.3          | 2.4           | 1.3         | 0.9        | 1.9    | 2.0      | 2.0         |     |
|  | 2014*                       | 5.2                        | 1.2          | 2.5           | 1.3         | 0.8        | 1.9    | 1.9      | 1.9         |     |
|  | 2015*                       | 4.3                        | 1.2          | 2.0           | 1.3         | 0.8        | 1.7    | 1.8      | 1.5         |     |
| $(E_{NO_x}^{Sat} - E_{NO_x}^{CEMS}) / E_{NO_x}^{CEMS}$ | 2005-2017                   | 10%                        | -22%         | 38%           | 20%         | -29%       | 21%    | 20%      | -56%        |     |
|  | 2006*                       | 6.1                        | 1.6          | 2.3           | 2.7         | 1.2        | 2.6    | 2.3      | 0.8         |     |
|  | 2007*                       | 5.9                        | 1.5          | 2.4           | 2.6         | 1.3        | 2.6    | 2.5      | 0.8         |     |
|  | 2008*                       | 5.6                        | 1.4          | 2.3           | 2.3         | 1.1        | 2.8    | 2.4      | 0.8         |     |
|  | 2009*                       | 4.1                        | 1.1          | 2.6           | 2.4         | 1.0        | 2.5    | 2.6      | 0.6         |     |
|  | 2010*                       | 3.7                        | 1.0          | 3.0           | 2.5         | 0.9        | 2.5    | 2.5      | 0.9         |     |
|  | 2011*                       | 3.4                        | 1.0          | 2.6           | 2.2         | 1.0        | 1.7    | 2.5      | 0.8         |     |
|  | 2012*                       | 3.3                        | 1.0          | 2.5           | 2.1         | 1.0        | 1.7    | 2.9      | 0.9         |     |
|  | 2013*                       | 3.1                        | 0.9          | 2.6           | 2.3         | 0.8        | 1.5    | 2.7      | 0.6         |     |
|  | 2014*                       | 2.5                        | 0.8          | 2.8           | 2.2         | 1.2        | 1.8    | 2.6      | 0.6         |     |
| $E_{CO_2}^{Sat}$<br>(Gg/h)                             | 2006*                       | 2.3                        | 0.9          | 2.4           | 1.8         | 1.1        | 1.7    | 1.7      | 0.5         |     |
|  | 2007*                       | 2.2                        | 1.4          | 1.4           | 1.6         | 1.0        | 2.0    | 1.7      | 0.8         |     |
|  | 2008*                       | 3.1                        | 1.5          | 1.7           | 2.4         | 1.9        | 2.2    | 1.8      | 1.2         |     |
|  | 2009*                       | 3.1                        | 1.5          | 1.7           | 2.4         | 1.8        | 2.2    | 1.9      | 1.2         |     |
|  | 2008*                       | 3.0                        | 1.5          | 1.6           | 2.4         | 1.8        | 2.2    | 1.8      | 1.2         |     |
|  | 2009*                       | 3.1                        | 1.4          | 1.5           | 2.3         | 1.7        | 2.1    | 1.9      | 1.3         |     |
|  | 2010*                       | 3.0                        | 1.4          | 1.4           | 2.2         | 1.7        | 2.1    | 1.9      | 1.4         |     |
|  | 2011*                       | 3.0                        | 1.3          | 1.3           | 2.1         | 1.5        | 2.0    | 2.0      | 1.4         |     |
|  | $E_{CO_2}^{CEMS}$<br>(Gg/h) | 2006*                      | 3.1          | 1.5           | 1.7         | 2.4        | 1.9    | 2.2      | 1.8         | 1.2 |
|  |                             | 2007*                      | 3.1          | 1.5           | 1.7         | 2.4        | 1.8    | 2.2      | 1.9         | 1.2 |
| 2008*  |                             | 3.0                        | 1.5          | 1.6           | 2.4         | 1.8        | 2.2    | 1.8      | 1.2         |     |
| 2009*  |                             | 3.1                        | 1.4          | 1.5           | 2.3         | 1.7        | 2.1    | 1.9      | 1.3         |     |
| 2010*  |                             | 3.0                        | 1.4          | 1.4           | 2.2         | 1.7        | 2.1    | 1.9      | 1.4         |     |
| 2011*  |                             | 3.0                        | 1.3          | 1.3           | 2.1         | 1.5        | 2.0    | 2.0      | 1.4         |     |

|       |  |           |     |      |     |     |      |     |     |      |
|-------|--|-----------|-----|------|-----|-----|------|-----|-----|------|
|       | 2012*  | 3.0       | 1.3 | 1.3  | 2.0 | 1.5 | 1.9  | 1.9 | 1.4 |      |
|       | 2013*  | 2.8       | 1.3 | 1.3  | 1.9 | 1.3 | 1.9  | 1.9 | 1.4 |      |
|       | 2014*  | 2.6       | 1.1 | 1.4  | 1.9 | 1.3 | 2.0  | 1.8 | 1.3 |      |
|       | 2015*  | 2.4       | 1.1 | 1.2  | 1.8 | 1.2 | 1.8  | 1.7 | 1.1 |      |
|       | 2016*  | 2.2       | 1.0 | 1.0  | 1.7 | 1.2 | 1.7  | 1.5 | 0.9 |      |
| <hr/> |  |           |     |      |     |     |      |     |     |      |
|       | $(E_{CO_2}^{Sat} - E_{CO_2}^{CEMS}) / E_{CO_2}^{CEMS}$ | 2005-2017 | 33% | -12% | 75% | 7%  | -30% | 4%  | 31% | -41% |

**Table 3** Summary of relative difference between satellite-derived NO<sub>x</sub> emissions ( $E_{NO_x}^{Sat}$ ) and bottom-up NO<sub>x</sub> emissions ( $E_{NO_x}^{CEMS}$ ), satellite-derived CO<sub>2</sub> emissions ( $E_{CO_2}^{Sat}$ ) and bottom-up CO<sub>2</sub> emissions ( $E_{CO_2}^{CEMS}$ ) for 8 US power plants during May to September from 2005 to 2017. The 3-year periods are represented by the middle year with an asterisk.

| Year  | <u>Relative Difference for NO<sub>x</sub></u> |                    | <u>Relative Difference for CO<sub>2</sub></u> |                    |
|-------|---|--------------------|---|--------------------|
|       | Mean  | Standard Deviation | Mean  | Standard Deviation |
| 2006* | 15%   | 29%                | 17%   | 39%                |
| 2007* | 10%   | 29%                | 16%   | 38%                |
| 2008* | 5%  | 30%                | 14%   | 39%                |
| 2009* | -3%   | 34%                | 6%  | 39%                |
| 2010* | -1%   | 38%                | 9%  | 46%                |
| 2011* | -5%   | 31%                | 3%  | 40%                |
| 2012* | -3%   | 31%                | 5%  | 41%                |
| 2013* | -4%   | 38%                | 4%  | 49%                |
| 2014* | -3%   | 36%                | 7%  | 46%                |
| 2015* | -8%   | 35%                | 2%  | 41%                |
| 2016* | -2%   | 29%                | 8%  | 22%                |